New observations of the topside ionosphere of Mars

Paul Withers, Martin Pätzold, Michael Mendillo, Silvia Tellmann, Bernd Häusler, Dave Hinson, and Len Tyler

(withers@bu.edu)

EGU07-A-09435 and XY0809

Tuesday 2007.04.17 10:30-12:00

EGU Meeting 2007, Vienna, Austria

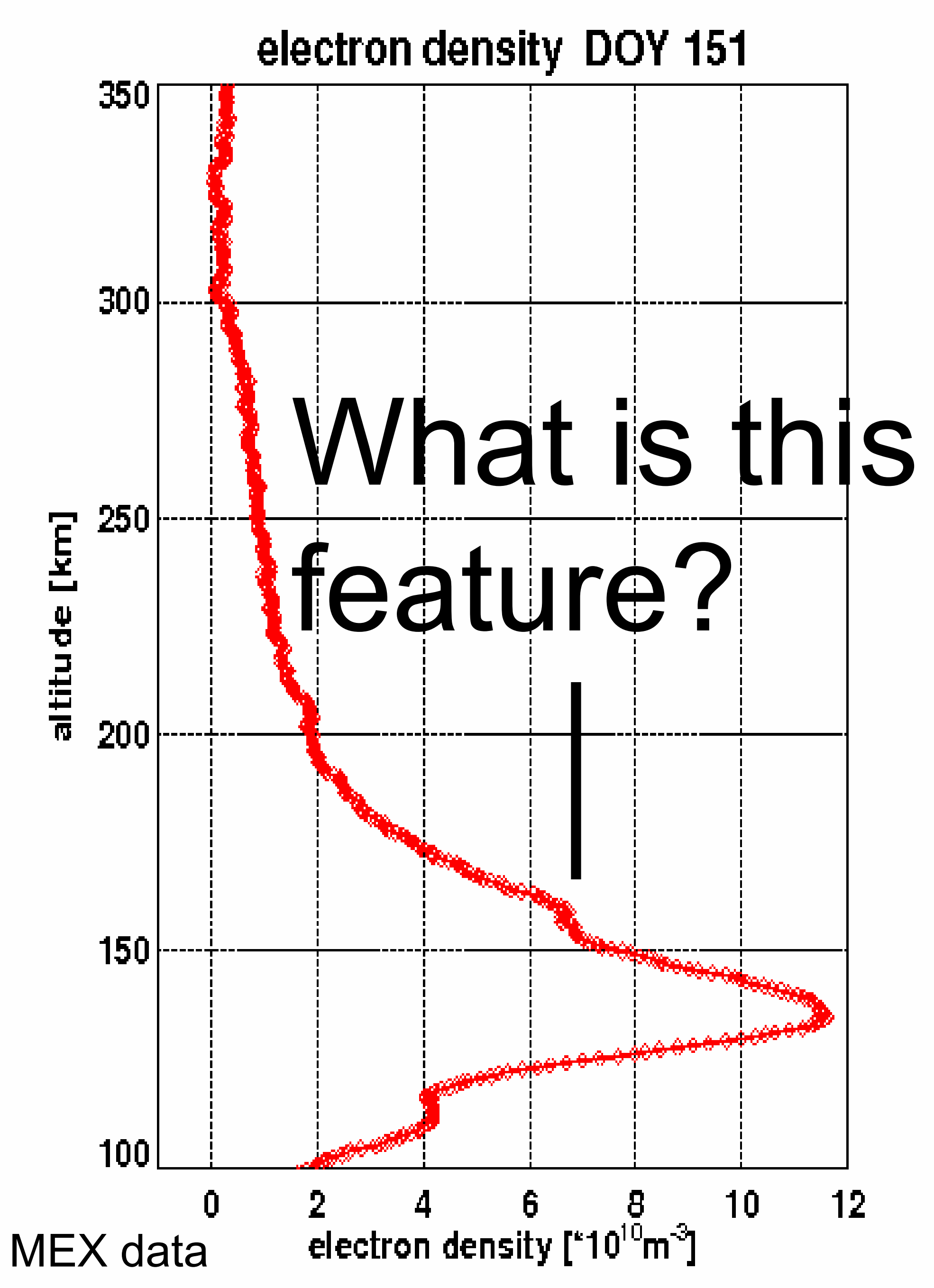

- A "step", or change in gradient, in electron density at ~160 km can be seen in MEX RS, MGS RS, and MEX MARSIS data.
- What is it?
- Why is it not apparent in Mariner 9, Viking Orbiter, or Viking Lander data?
- Why is it not predicted by models?

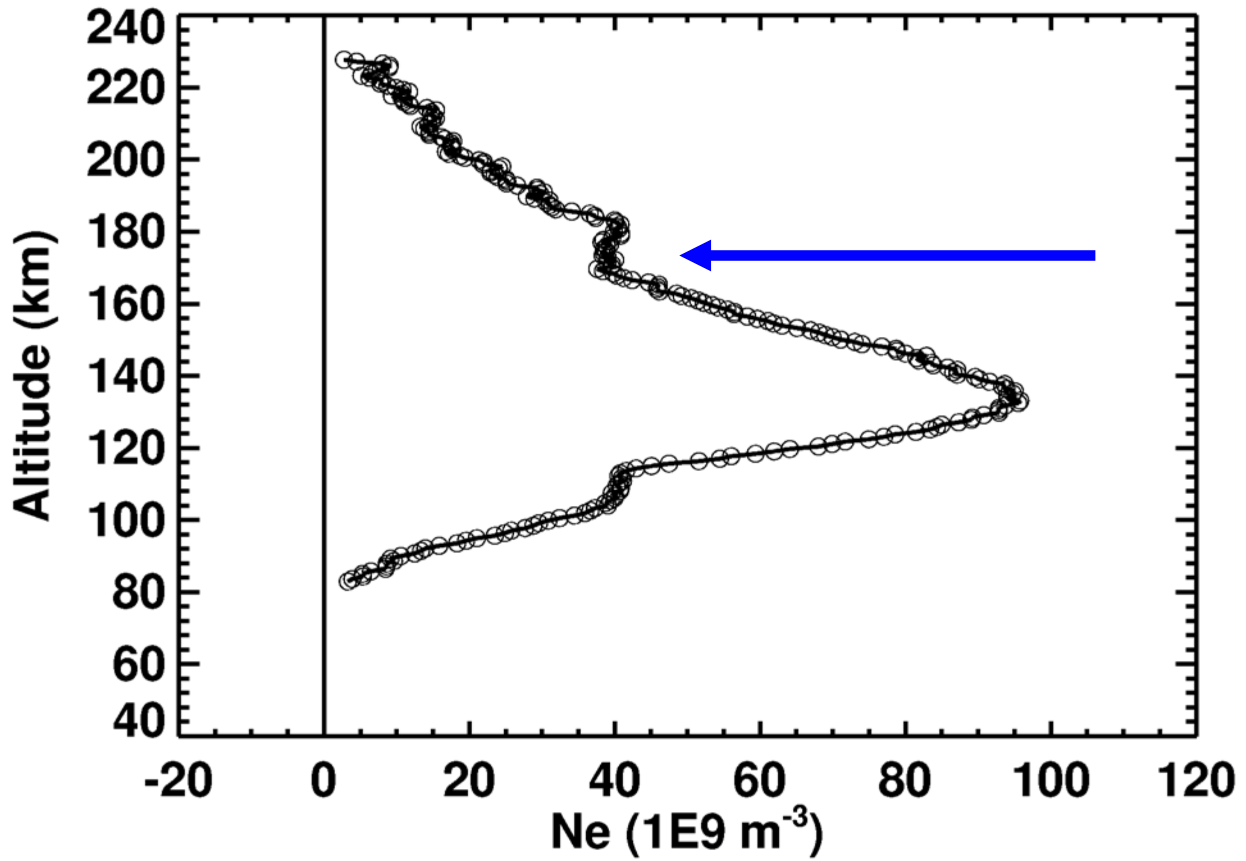

MGS
3084V55A.EDS
2003-03-25
Lat = 80N
LST = 12.6 hrs
SZA = 71 deg

This “step” is visible in many MGS profiles

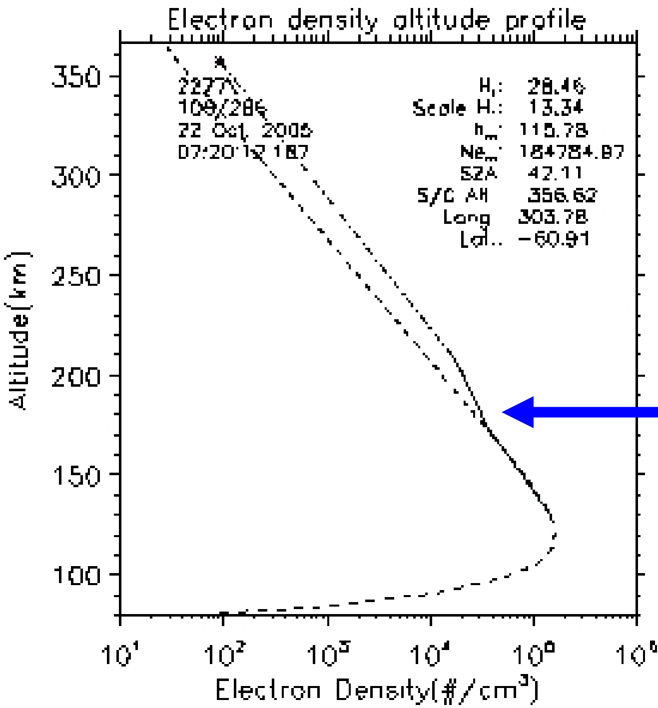

OF VERTICAL REFLECTIONS FROM THE TOPSIDE MARTIAN IONOSPHERE

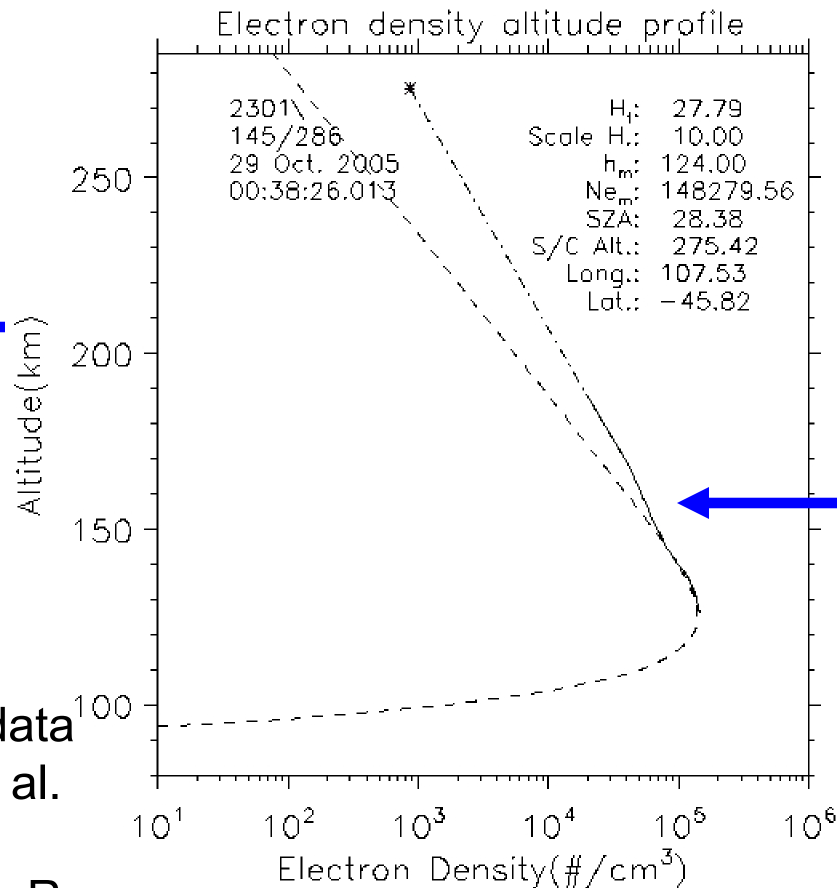

MARSIS is a topside ionospheric sounder on Mars Express.

It also sees a “step” in the topside

MARSIS data
Nielsen et al. (2006)
Space Sci. Rev.

Figure 6. The solid and dash-dot curve is the estimated profile of the top side electron densities derived using the lamination technique. The solid curve covers the densities for which echoes were observed, and the dash-dot curve the assumed exponential decrease. Note, the dash-dot curve starts at the derived electron density (star) at the height of the spacecraft. The dashed curve is a Chapman layer fitted to the observations. In the plot is noted the associated maximum electron density (148279 el/cm^3) and altitude of the maximum ($\sim$124 km) in the sub solar region, together with the neutral scale height (10.0 km), a top-side scale height ($\sim$28 km), and solar zenith angle ($\sim$28 degrees).

Typical Ionospheric Profiles for Earth and Mars

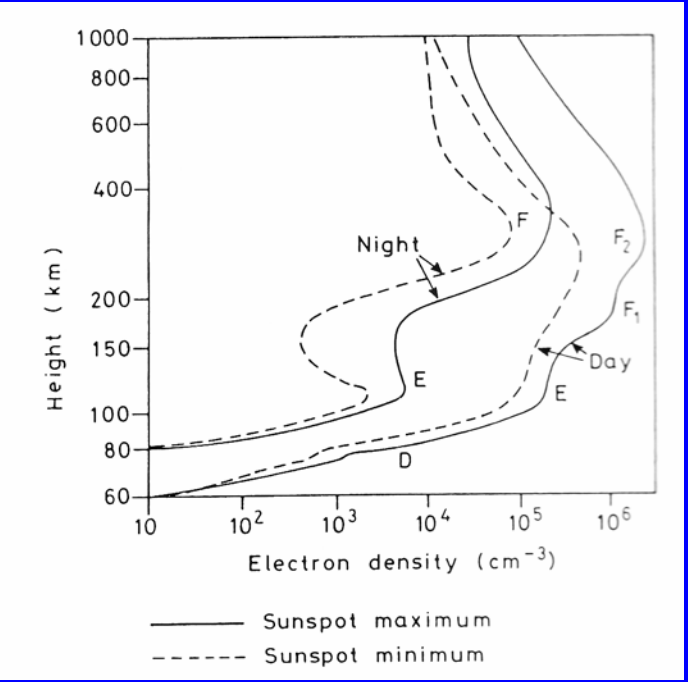

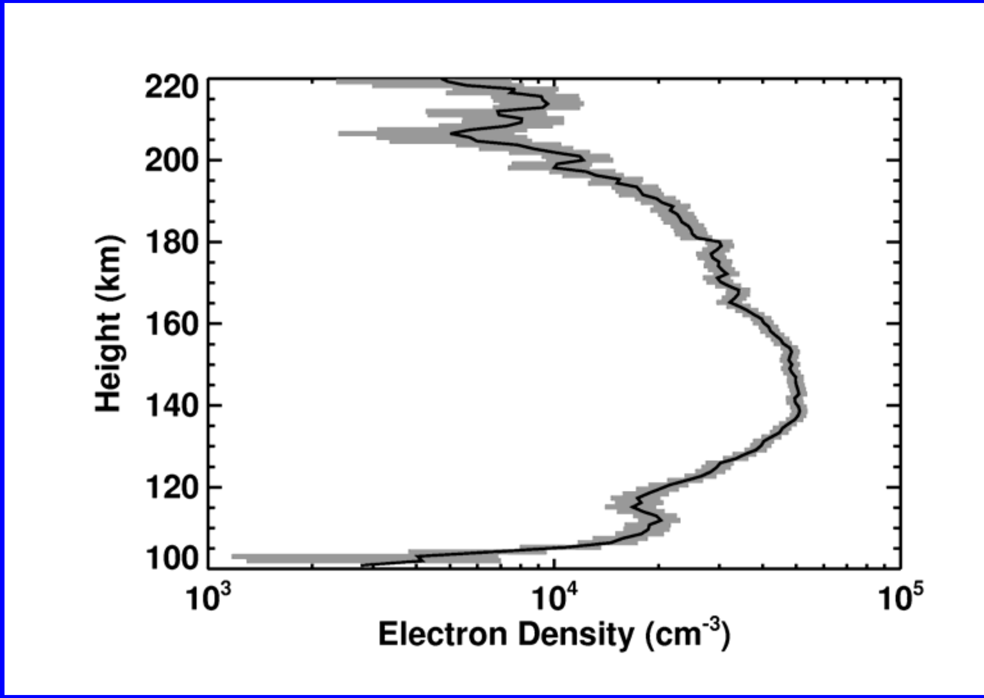

Earth (Hargreaves, 1992)
F layer due to EUV photons
E layer due to soft X-rays
D layer due to hard X-rays

Soft ~ 10 nm, hard ~ 1 nm

Mars (MGS RS data)
Transport important above ~180 km
Main peak at 140 km due to EUV photons
Lower peak at 110 km due to X-rays. Lower peak is very variable and often absent

Mars ionospheric chemistry

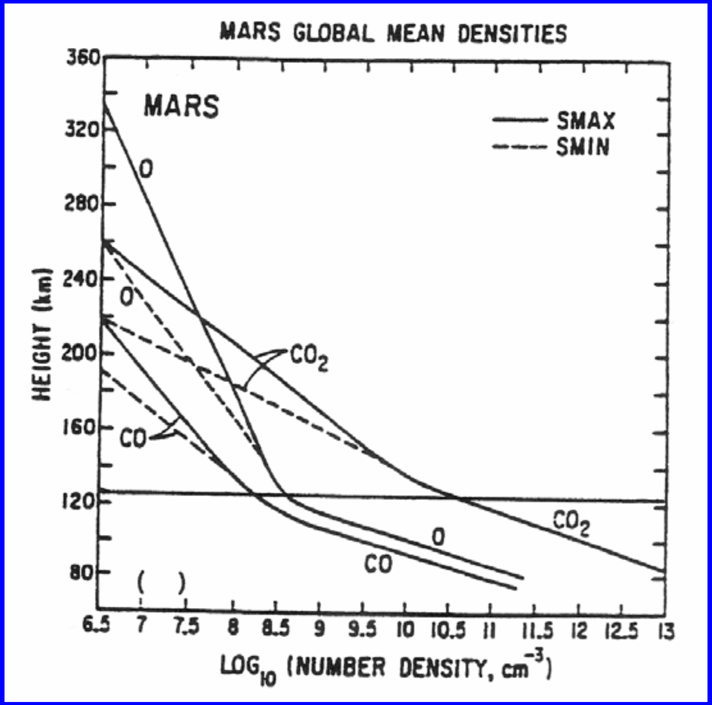

Bougher et al., 2002

- CO_2 + hv -> CO_2^+ + e (production)
- CO_2^+ + O -> O_2^+ + CO (chemistry)
- O_2^+ + e -> O + O (loss)

- The presence of neutral O affects ionospheric chemistry and electron densities

- Few observations of neutral atmosphere composition exist
- O/CO_2 ratio is predicted to vary with altitude, season, time of day, etc
- This is a challenge for ionospheric modelling and data analysis

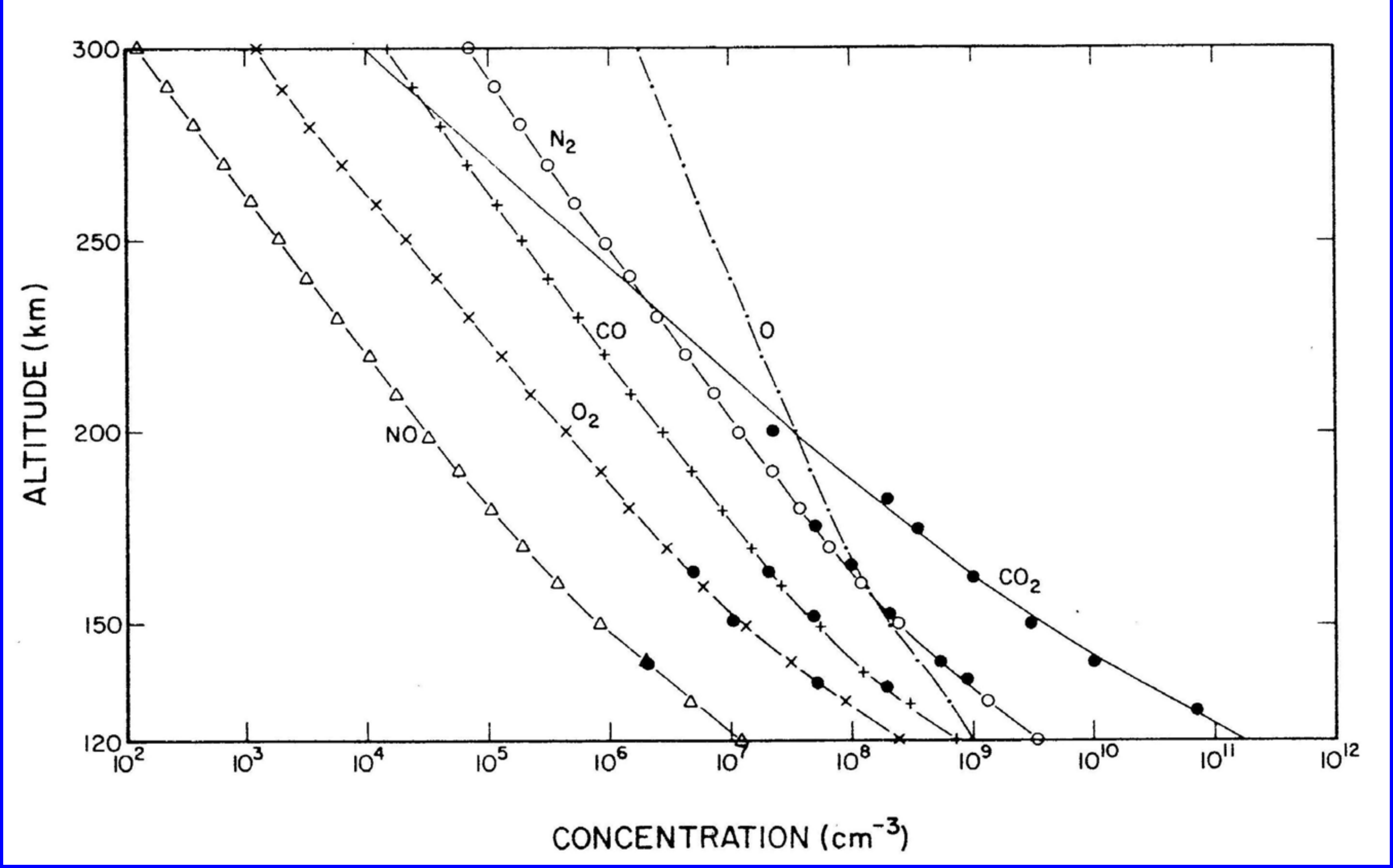

Data and model for Mars atmospheric composition from Viking 1.
Hanson et al. (1977) and Nier and McElroy (1977)

Planetary Properties at Ionospheric Peak

	Venus	Earth E-region	Mars
g (m s^{-2})	8.9	9.8	3.7
Solar distance (AU)	0.7	1.0	1.4 – 1.7
z_{peak} (km)	140	110	120
Neutrals	CO_2	N_2, O_2	CO_2
Ions	O_2^+	O_2^+, NO^+	O_2^+
Production process	CO_2+hv -> CO_2^+ + e CO_2^++O -> CO + O_2^+	N_2+hv -> N_2^+ + e N_2^+ + O -> N + NO^+ O_2+hv -> O_2^+ + e	CO_2+hv -> CO_2^+ + e CO_2^++O -> CO + O_2^+
Loss process	Dissociative Recombination	DR	DR
N_n (cm^{-3})	1 E 11	1 E 13	1 E 11
N_e (cm^{-3})	7 E 5	1 E 4	2 E 5
T_n (K)	200	300	200
T_e (K)	1000	300 – but ~1000 at 150 km	200

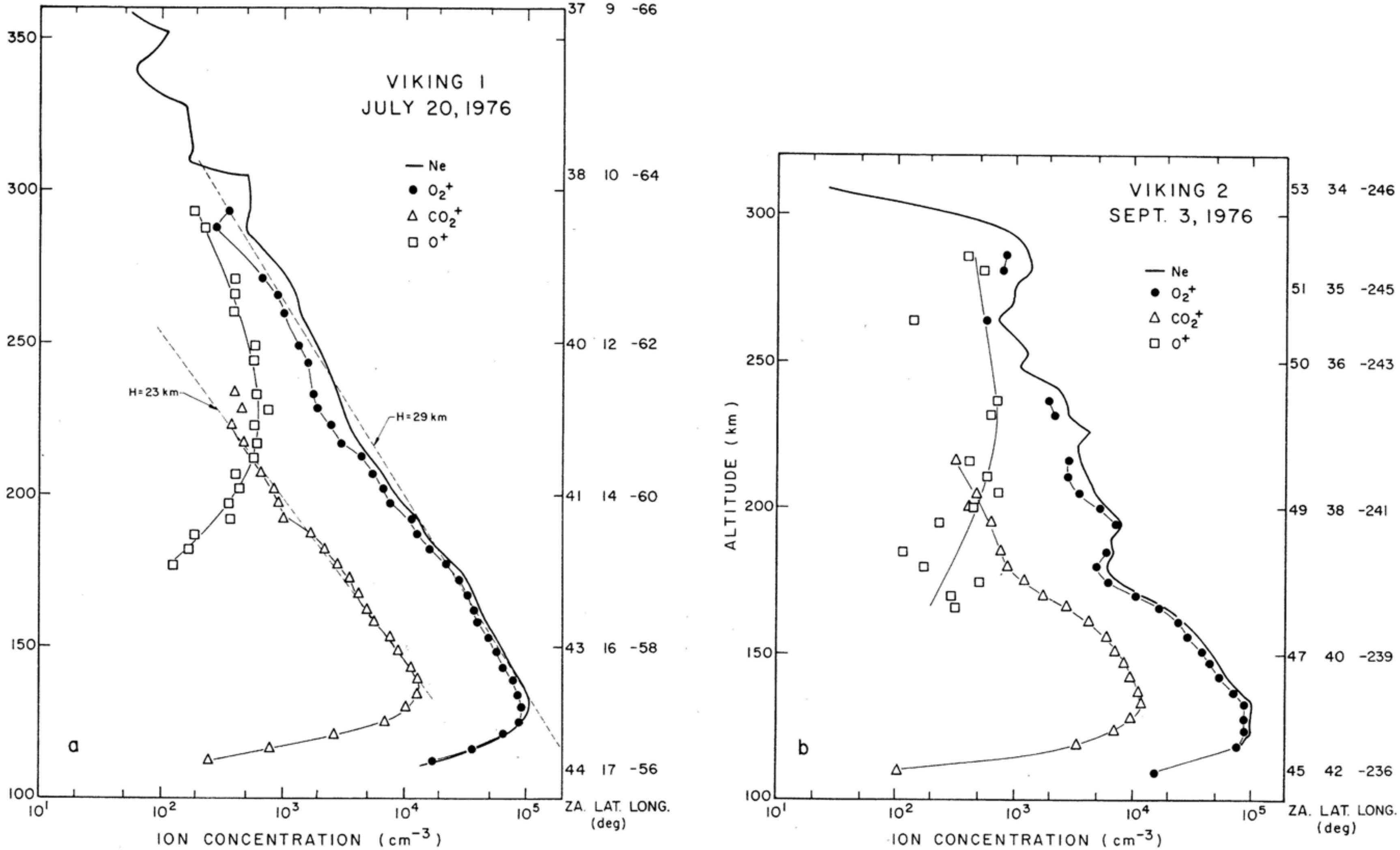

Fig. 6. Plots of observed ion concentrations versus altitude. The solid lines labeled N_e represent the sum of the individual ion concentrations. The dashed lines in Figure 6*a* are eyeball fits to the CO_2^+ and O_2^+ (N_e) data and correspond to the scale heights shown. At the right of each plot the solar zenith angle and sublander Mars coordinates are shown at several altitudes.

The only observations of Mars ionospheric composition (Hanson et al., 1977)

No “step” or similar feature is visible on the topside

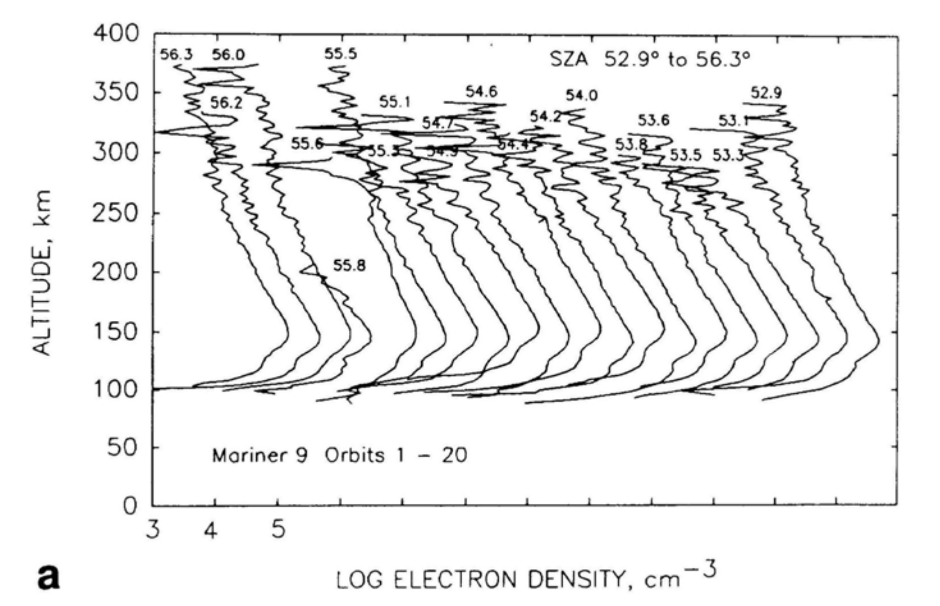

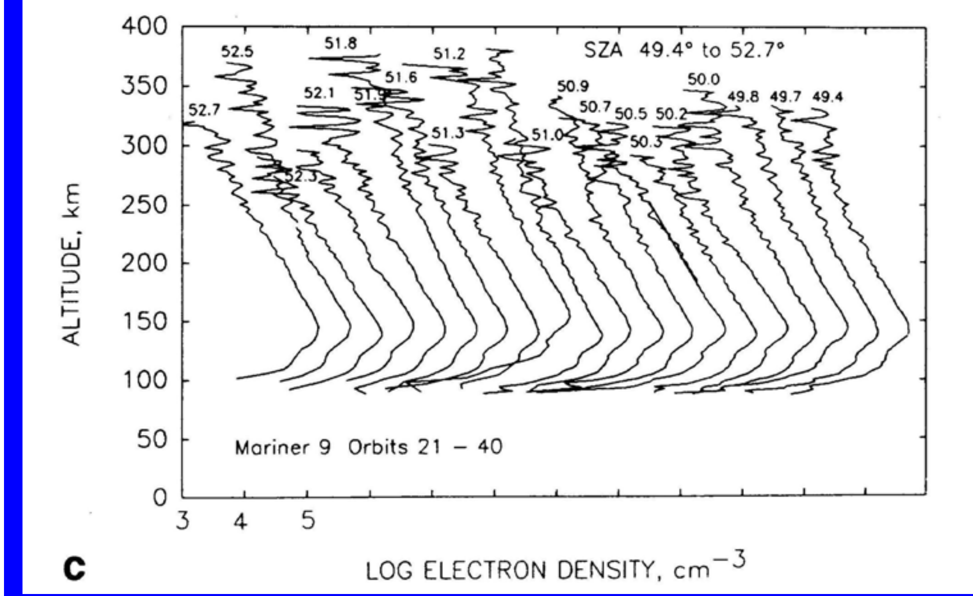

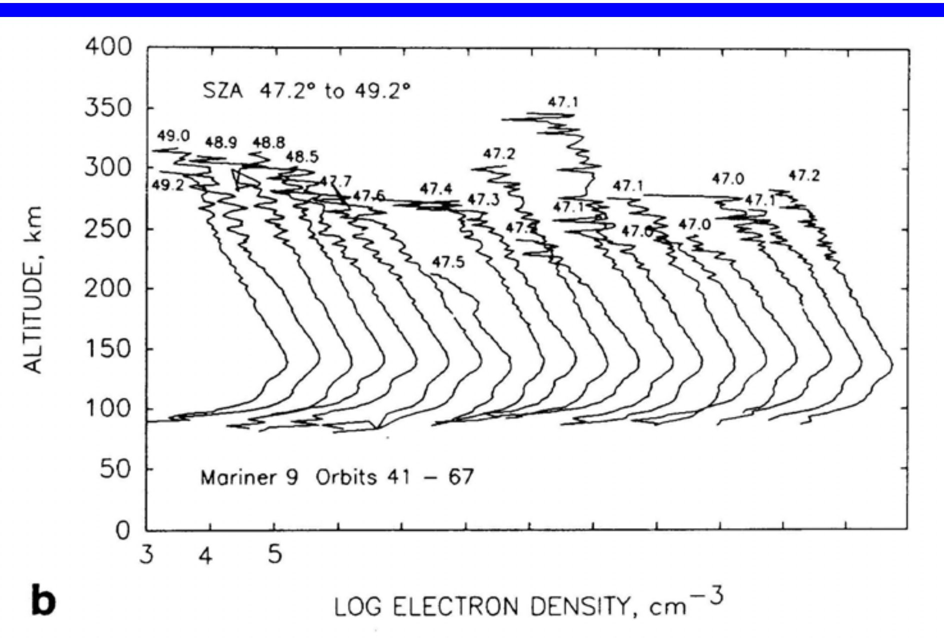

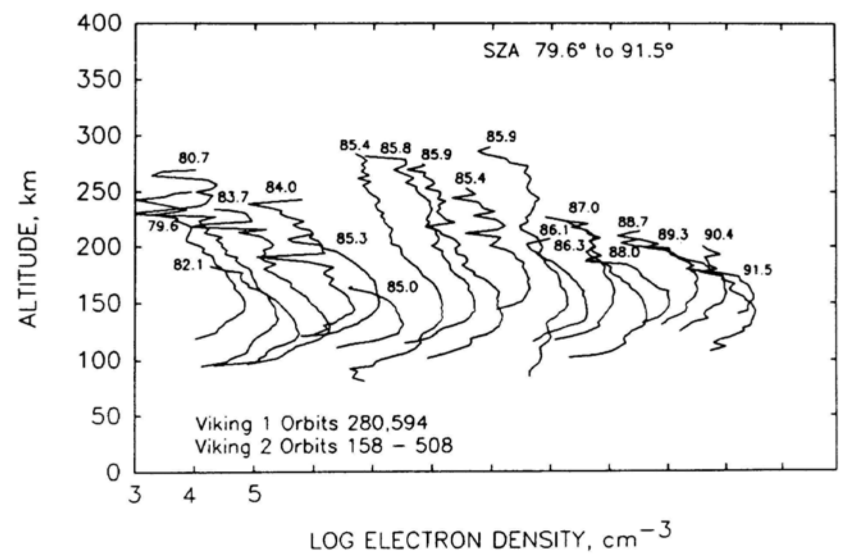

Fig. 6. Vertical electron density profiles in the Mars ionosphere as observed with Viking 1 and Viking 2 at high solar zenith angles, which are shown above each profile.

Mariner 9 and Viking Orbiter radio occultation electron density profiles (Kiore 1992). No obvious "steps" are visible.

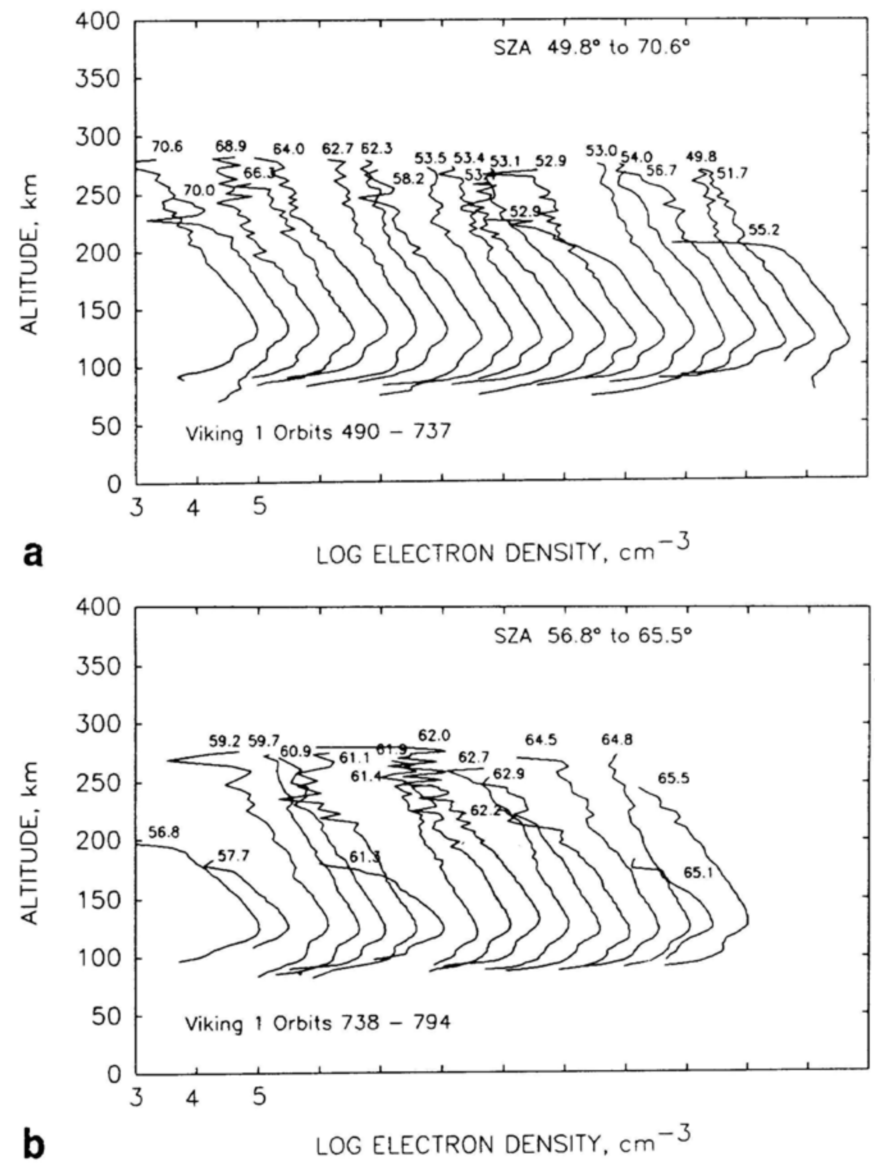

Fig. 3. Vertical electron density profiles in the Mars ionosphere as observed with Viking 1 in 1976. (a) Orbits 490-737; (b) Orbits 738-794. Solar zenith angles are shown next to each profile.

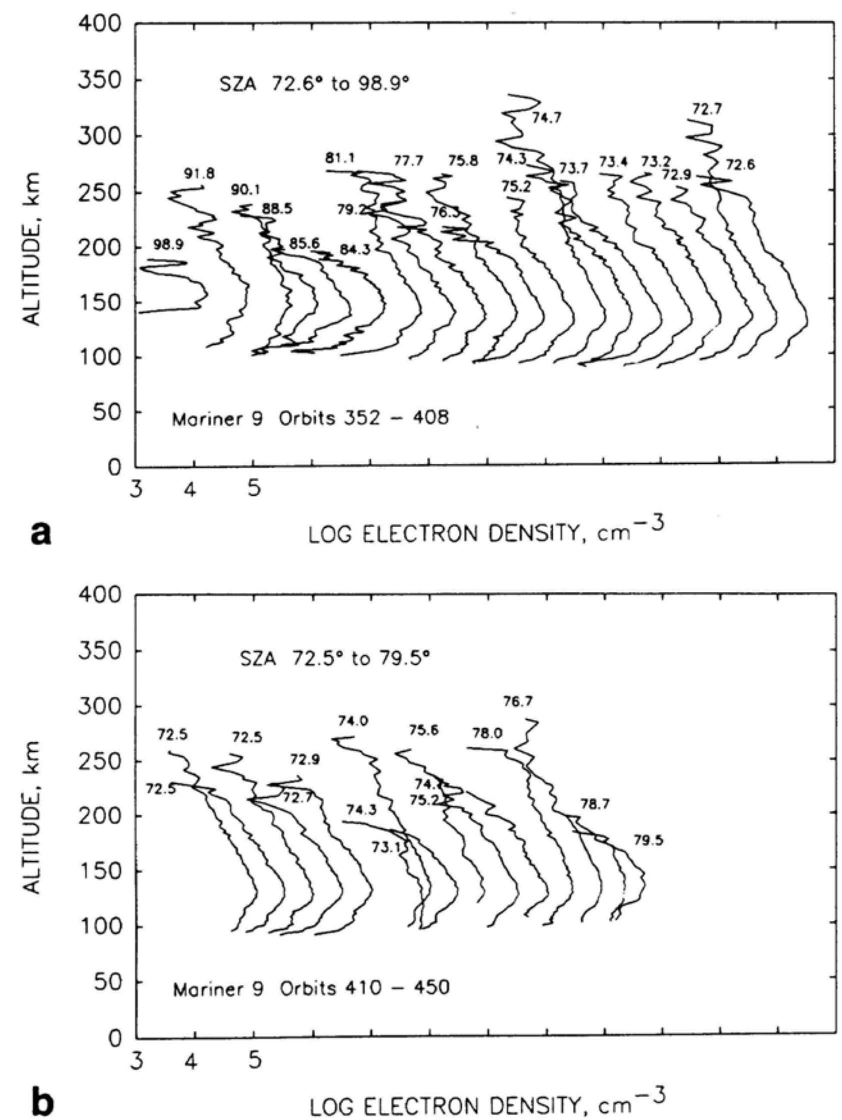

Fig. 5. Vertical electron density profiles in the Mars ionosphere as observed with Mariner 9 in 1972. (a) Orbits 352-408; (b) Orbits 410-450. Solar zenith angles are shown above the profiles.

Mariner 9 and Viking Orbiter radio occultation
electron density profiles (Kiore 1992). No obvious “steps” are visible.

Geophysical Research Abstracts, Vol. 9, 09435, 2007
SRef-ID: 1607-7962/gra/EGU2007-A-09435

New observations of the topside ionosphere at Mars

P. Withers (1), M. Pätzold (2), M. Mendillo (1), S. Tellmann (2), B. Häusler (3), D. Hinson (4) and G. L. Tyler (4)

(1) Center for Space Physics, Boston University, USA, (2) Institut für Geophysik und Meteorologie, Universität zu Köln, Germany, (3) Institut für Raumfahrttechnik, Universität der Bundeswehr München, Neubiberg, Germany, (4) Department of Electrical Engineering, Stanford University, USA (withers@bu.edu / Fax: +1 617 353 6463)

The daytime Martian ionosphere consists of a main layer M2 at typically 135 km altitude and a secondary layer M1 at 110 km altitude, both formed by solar radiation at EUV and X-ray, respectively. The peak altitudes and peak densities vary according to the diurnal changes in solar zenith angle as expected when under solar control. These layers are controlled by photochemical processes and can be represented as Chapman layers. However, the topside ionosphere is more complex and difficult to model. It is affected by plasma transport due to dynamical processes and changing ion chemistry (increasing amounts of O+ ions, as observed by the Viking Landers). New Mars Express Radio Science experiment MaRS observations show the transition from the region around the photochemically-controlled EUV peak, which is effectively an O2+ Chapman layer, to the topside in great detail. We discuss how these observations can be used to better understand the complex topside ionosphere, relating them to Mars Global Surveyor observations and predictions from numerical models. Vertical profiles of excess topside electron density have shapes that resemble a Chapman function. We shall investigate whether these shapes are caused by photochemical processes or the transition to a transport-dominated region.

Chen et al. (1978)

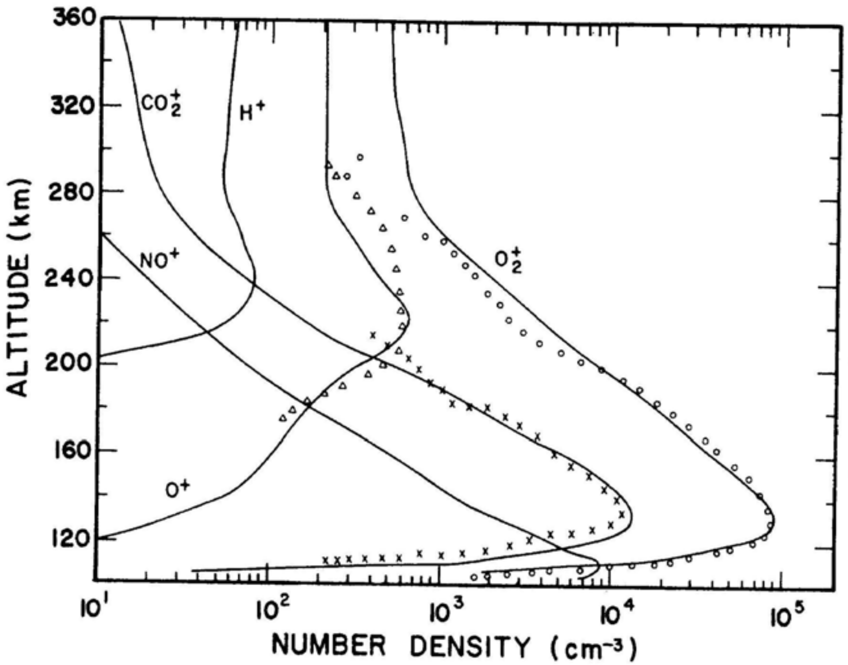

Fig. 6. Ion density profiles. The solid lines are calculated profiles with outward diffusive velocity upper boundary conditions of 1 km s^{-1} for all ions except H^+, which was 10 km s^{-1}. The circles are O_2^+ data, the triangles are O^+ data, and the crosses are CO_2^+ data, all being from the Viking 1 RPA experiment [*Hanson et al.*, 1977].

Viking-era models do not show any topside “step”.

1-D models include photochemistry and vertical transport by diffusion. “Transport processes begin to control the ion density distribution at altitudes above 200 km.” (Chen et al., 1978)

Hanson et al. (1977)

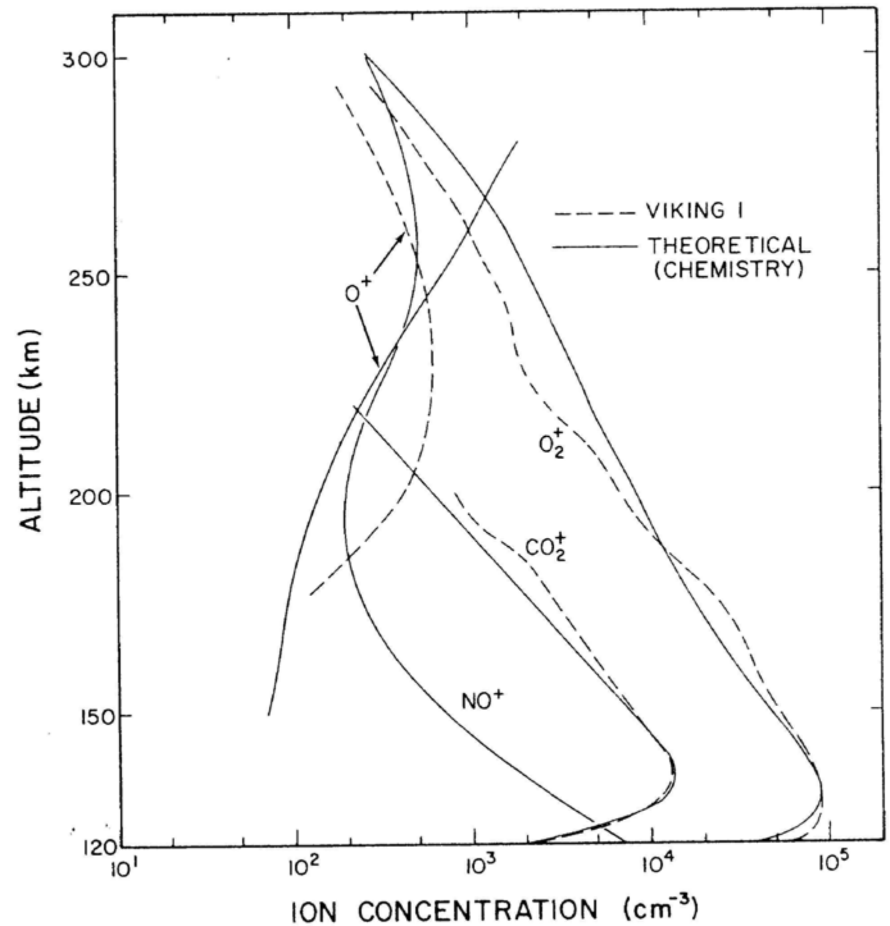

Fig. 11. A comparison of the measured ion concentration from Viking 1 profiles and a theoretical model ionosphere in chemical equilibrium. Only ions with concentrations greater than 200 ions cm^{-3} are plotted. NO^+ could not be uniquely identified from the RPA data.

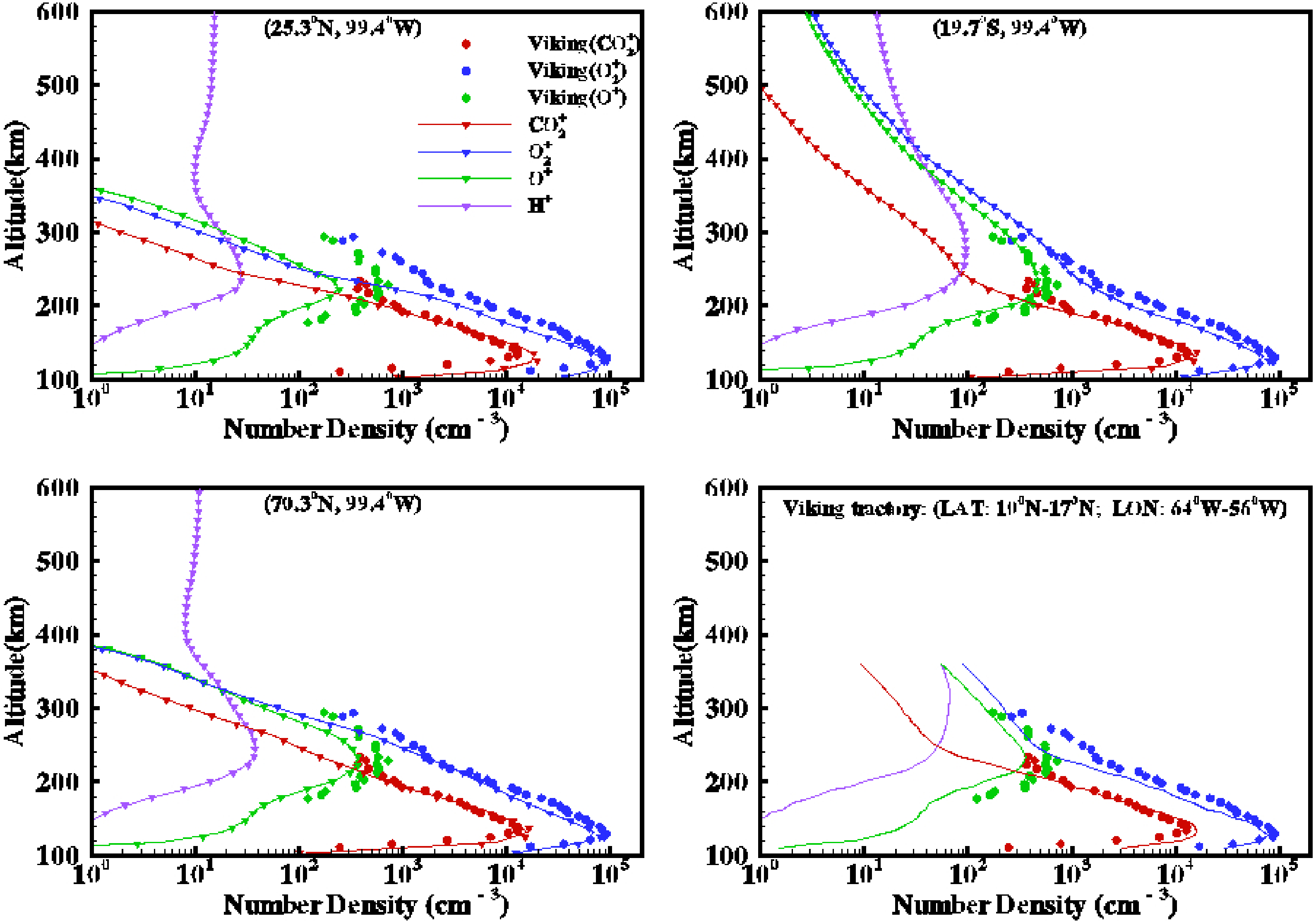

Figure 8. The calculated solar cycle minimum density profiles for case 4 along radial lines for different latitudes in the X-Z plane compared with Viking observation.

Recent MHD models do not show a topside "step" (Ma et al., 2004)

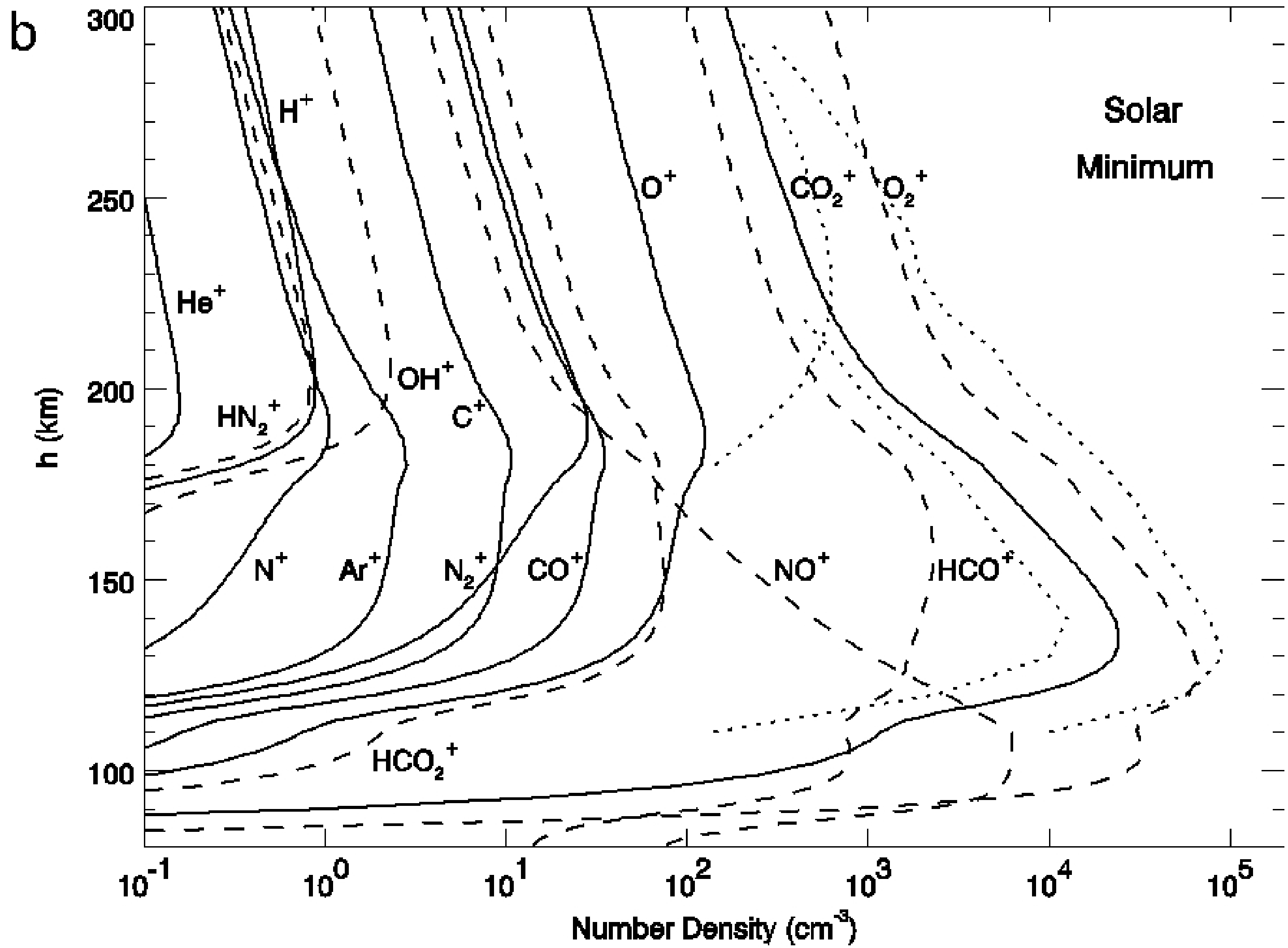

Figure 1. Composition of Mars' upper atmosphere (a) and ionosphere (b) at low solar activity. Primary ions are shown by solid lines, secondary ions by dashed lines. Dotted lines are the Viking 1 measurements of O^+, CO_2^+, and O_2^+ (from left to the right).

Recent 1-D photochemistry/diffusion models do not show a "step", although this figure does hint at interesting behaviour at 180 km. SZA=60 degrees. Krasnopolsky (2002)

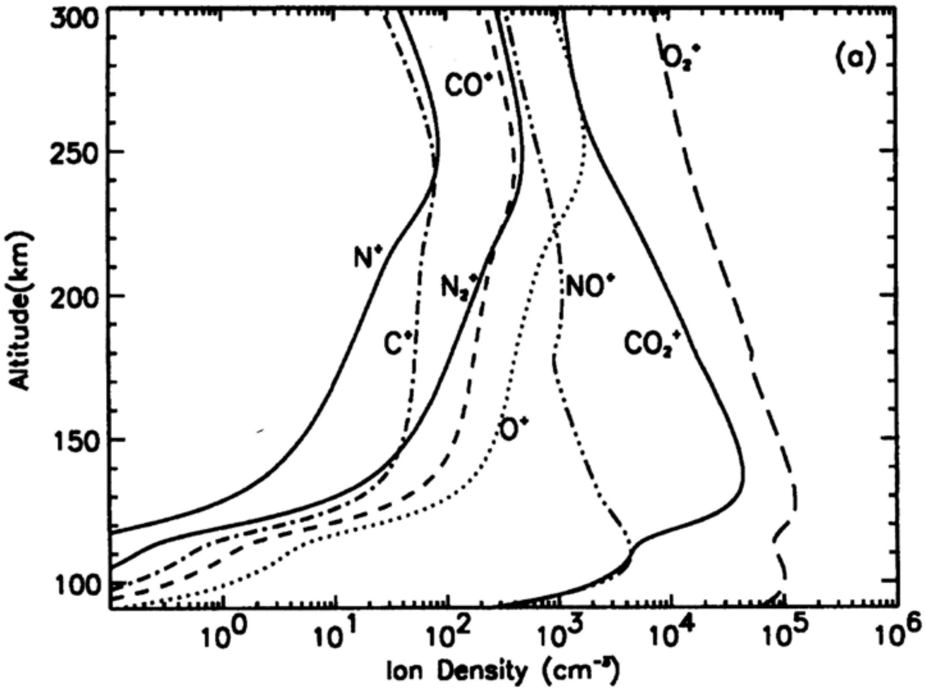

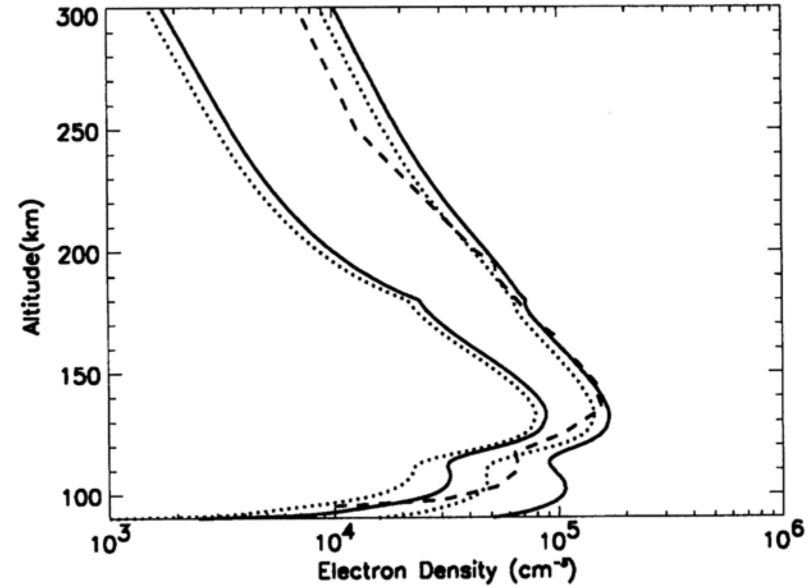

Fig. 9. Predicted electron density profiles for the low and high solar activity models. The larger densities are from the high solar activity model and the smaller are from the low solar activity model. The solid curves were computed using solar fluxes from Tobiska /10/,and the dotted curves were computed with solar fluxes from Hinteregger /12,13/. The dashed curve is the electron density profile derived from the Mariner 6 radio occultation measurements /29/.

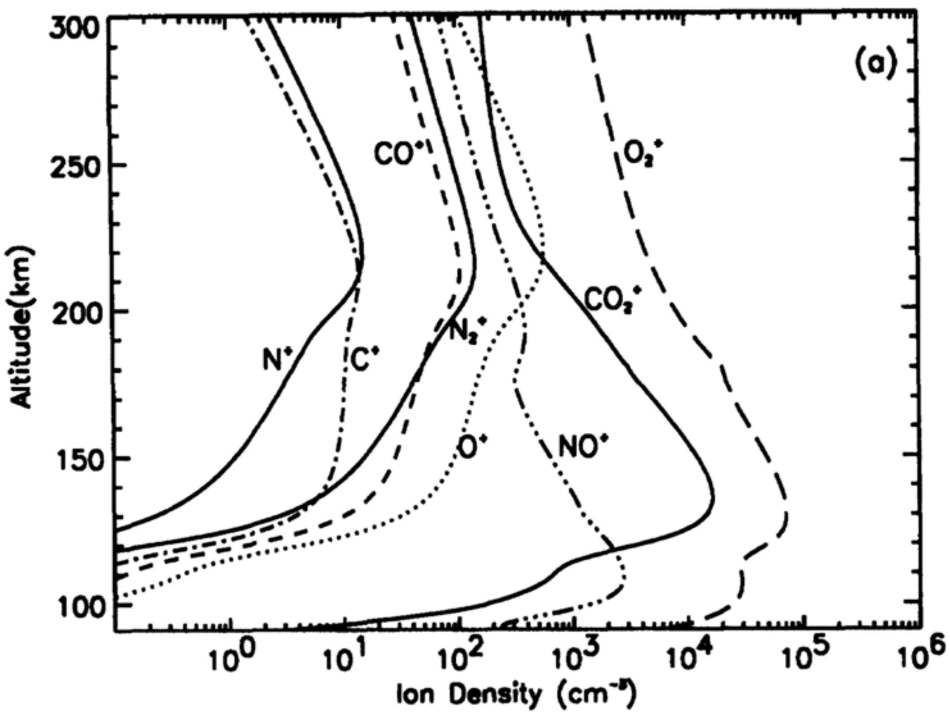

Another recent 1-D photochemistry/ diffusion model shows something happening at 180 km, but does not show the topside “step”.

Top left: High solar activity
Bottom left: Low solar activity

SZA = 60 degrees
Fox et al. (1996)

MGS RS data
3012G12A.EDS
2003-01-12
Lat = 76N
LST = 04.4 hrs
SZA = 75 deg

Open black circles = Observed Ne(z)

Red curves = Two Chapman fits
First fit to X-ray peak in observed Ne(z)
Second fit to residual after first fit subtracted from observed Ne(z)

Green curve = Sum of two Chapman fits

Blue curve = Residual after both fits subtracted from observed Ne(z)

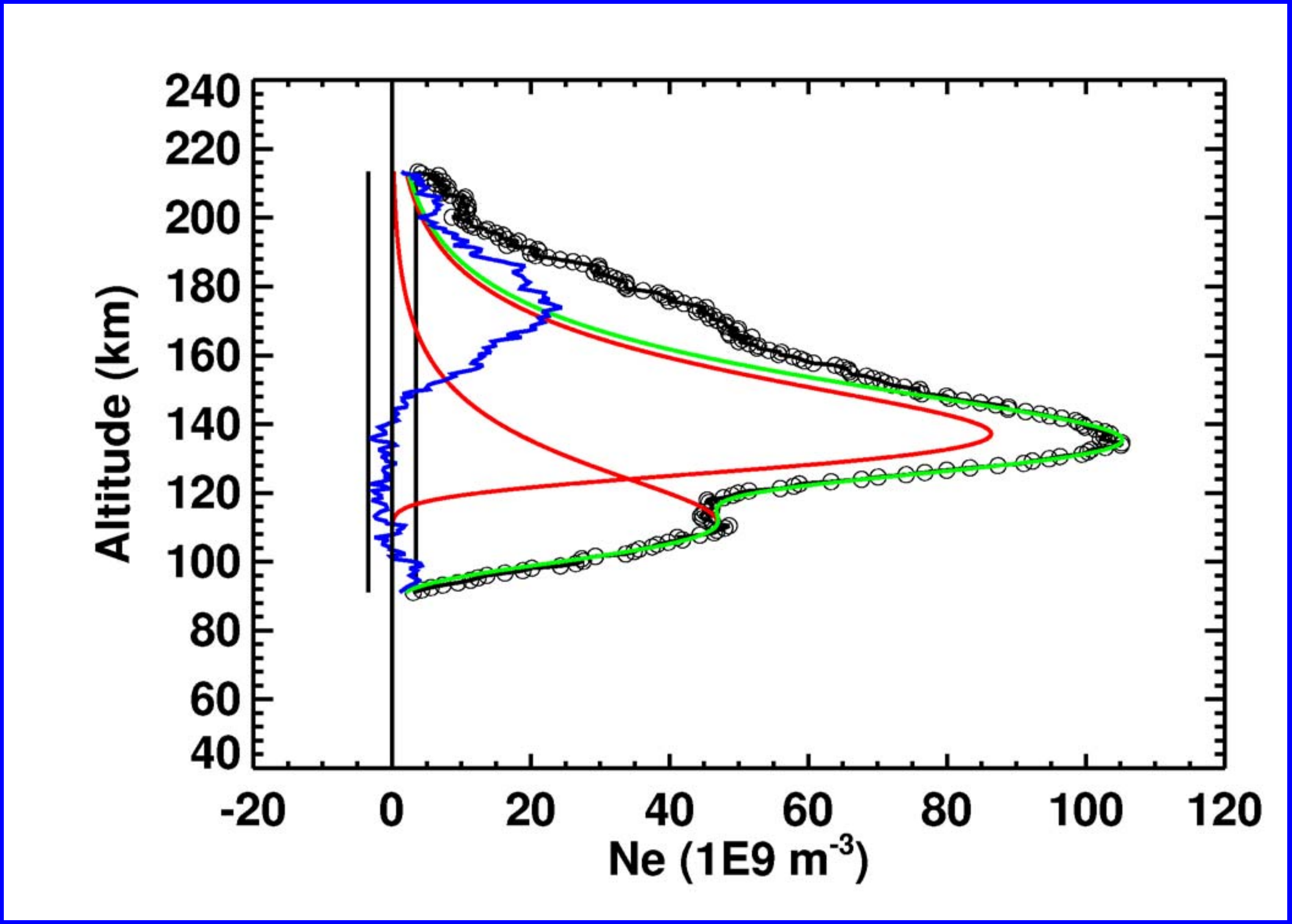

After fits to the X-ray and EUV ionospheric layers are removed, excess electron density in the topside is visible around 175 km.

MGS RS data
3012G12A.EDS
2003-01-12
Lat = 76N
LST = 04.4 hrs
SZA = 75 deg

Peak altitude, peak electron density, and neutral scale height for three fitted Chapman layers:

112 km, 47 m^{-3}, 9 km
137 km, 86 m^{-3}, 9 km
173 km, 22 m^{-3}, 10 km

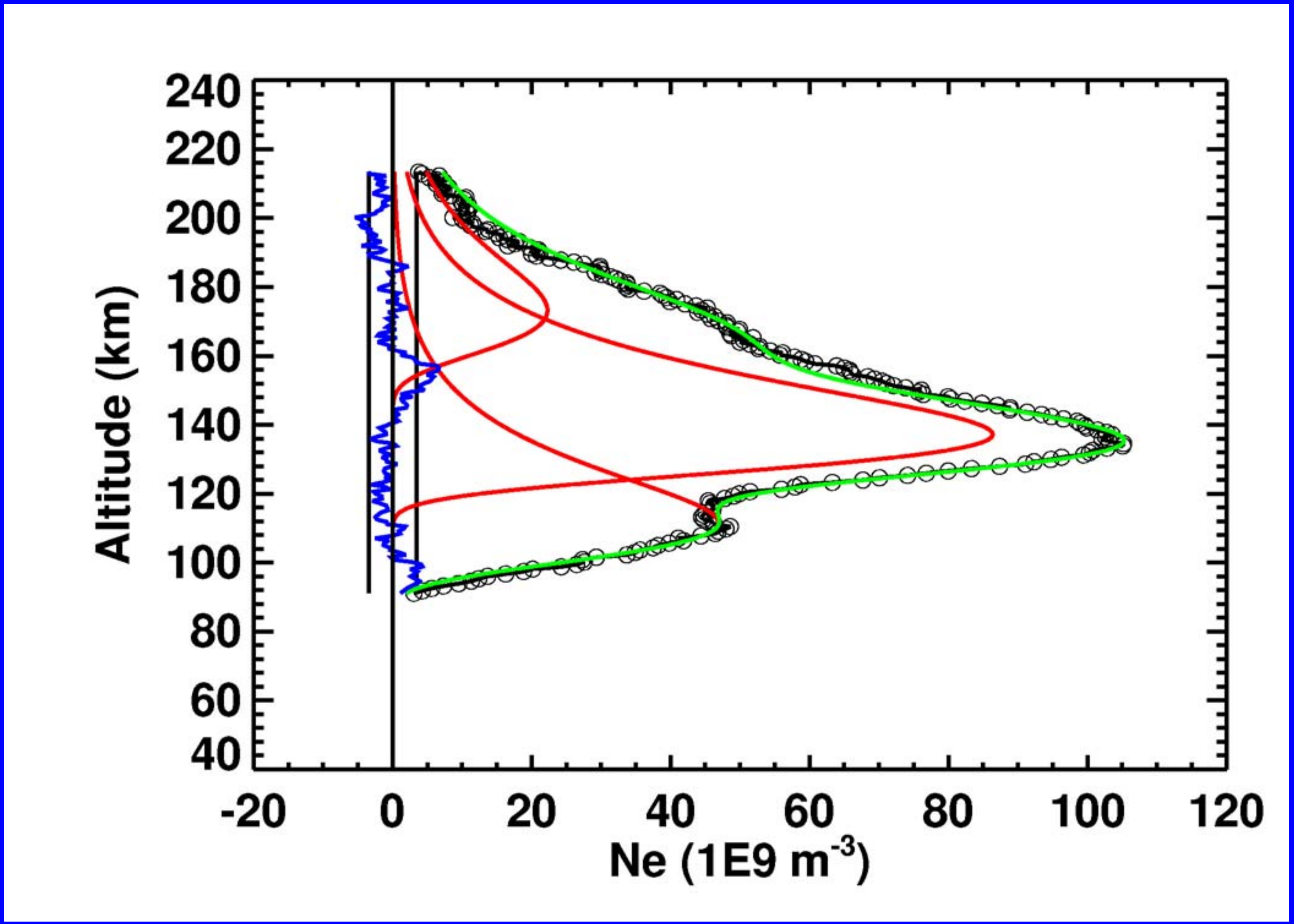

The sum of three Chapman layers (green curve) is a good match to the observed Ne(z) (open black circles). The residuals (blue curve) are consistent with the uncertainties in the observed Ne(z) (vertical black lines).

MGS RS data
3081P28A.EDS
2003-03-22
Lat = 81N
LST = 12.4 hrs
SZA = 71 deg

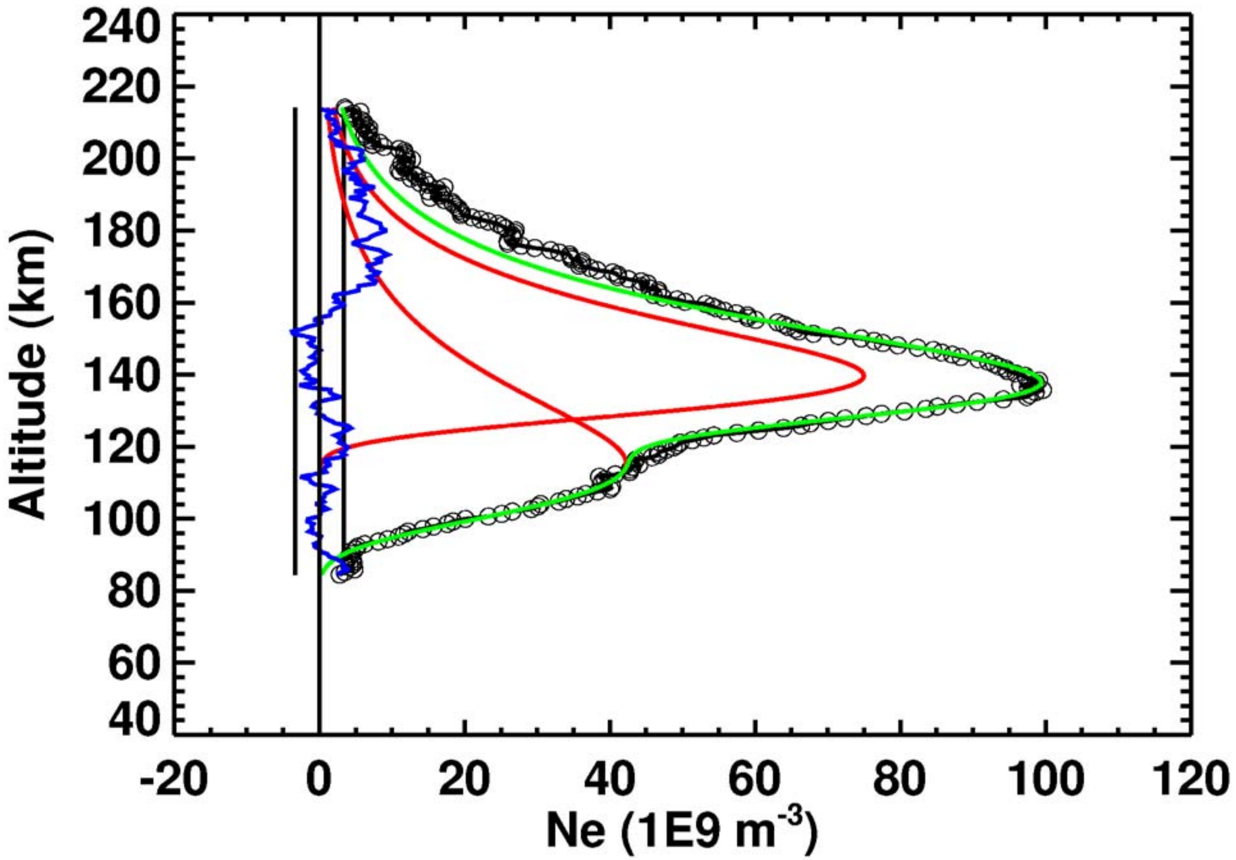

Open black circles = Observed Ne(z)

Red curves = Two Chapman fits
First fit to X-ray peak in observed Ne(z)
Second fit to residual after first fit subtracted from observed Ne(z)

Green curve = Sum of two Chapman fits

Blue curve = Residual after both fits subtracted from observed Ne(z)

After fits to the X-ray and EUV ionospheric layers are removed, excess electron density in the topside is visible around 180 km.

MGS RS data
3081P28A.EDS
2003-03-22
Lat = 81N
LST = 12.4 hrs
SZA = 71 deg

Peak altitude,
peak electron density,
and neutral scale
height for three fitted
Chapman layers:

115 km, 42 m^{-3}, 12 km
140 km, 75 m^{-3}, 9 km
174 km, 7.8 m^{-3}, 11 km

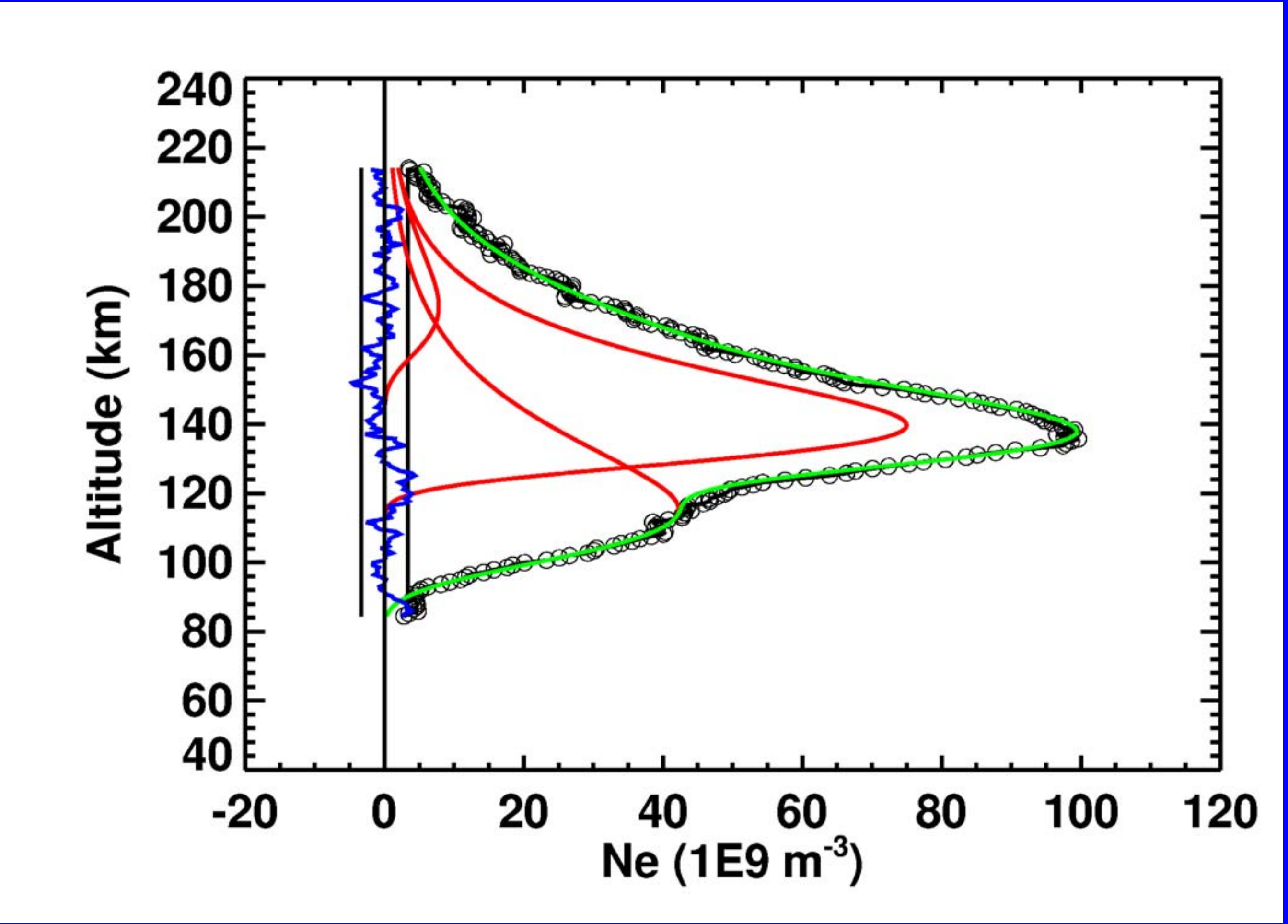

The sum of three Chapman layers (green curve) is a good match to the observed Ne(z) (open black circles). The residuals (blue curve) are consistent with the uncertainties in the observed Ne(z) (vertical black lines).

MEX RS data
2005-12-31 Orbit 2528
Lat = 61.0N Lon = 211E
LST = 13:24 hrs Ls = 349.2 deg
SZA = 67.7 deg

In this example production functions are added together
Ne proportional to square root(PF)

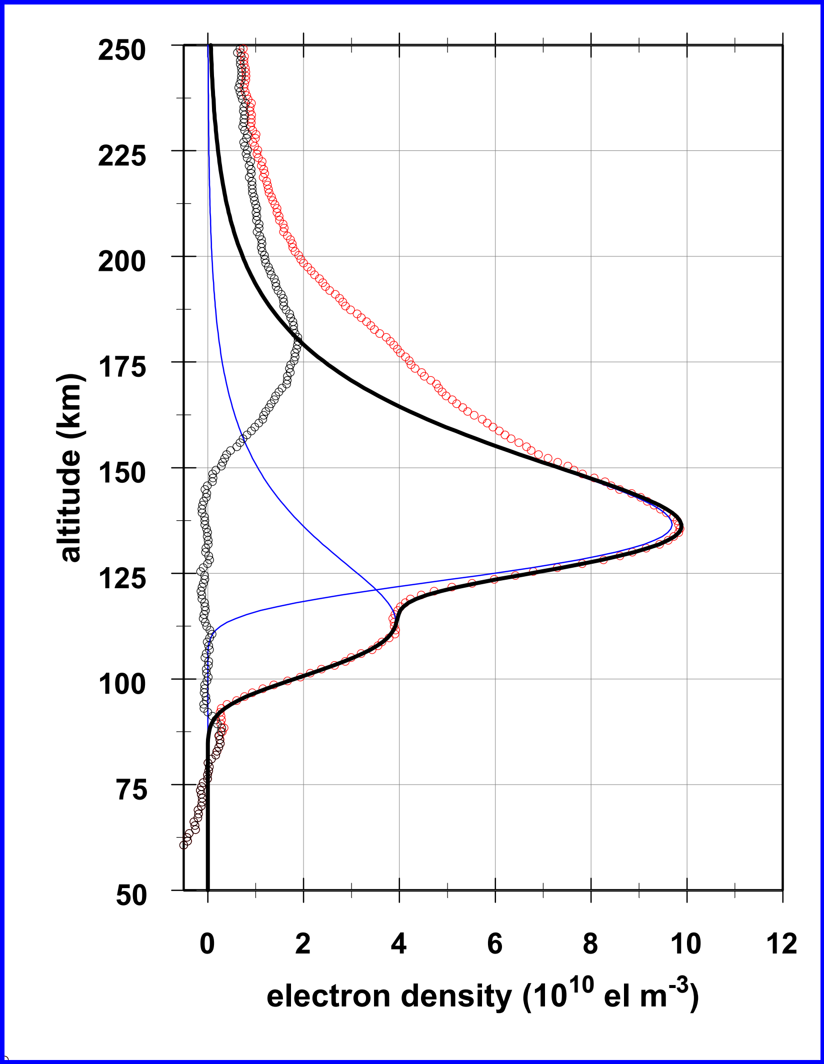

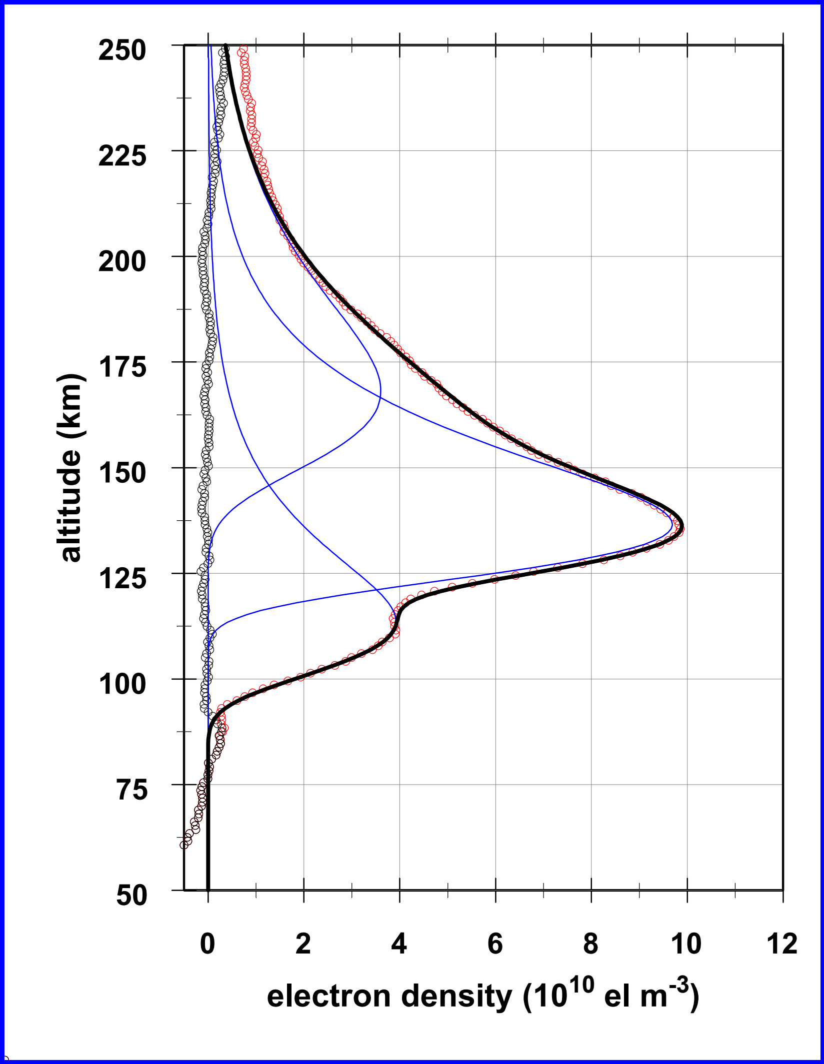

MEX RS data
2006-01-01 Orbit 2531
Lat = 60.7N Lon = 277E
LST = 13:26 hrs Ls = 349.7 deg
SZA = 67.3 deg

In this example production functions are added together
Ne proportional to square root(PF)

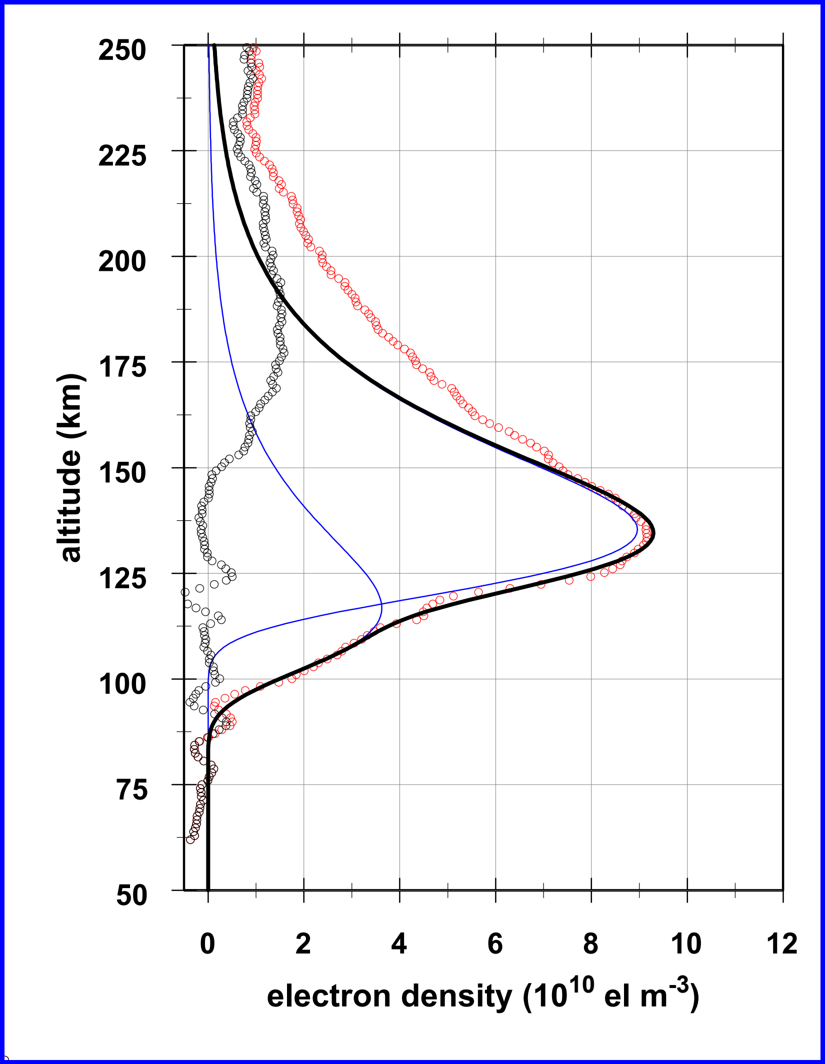

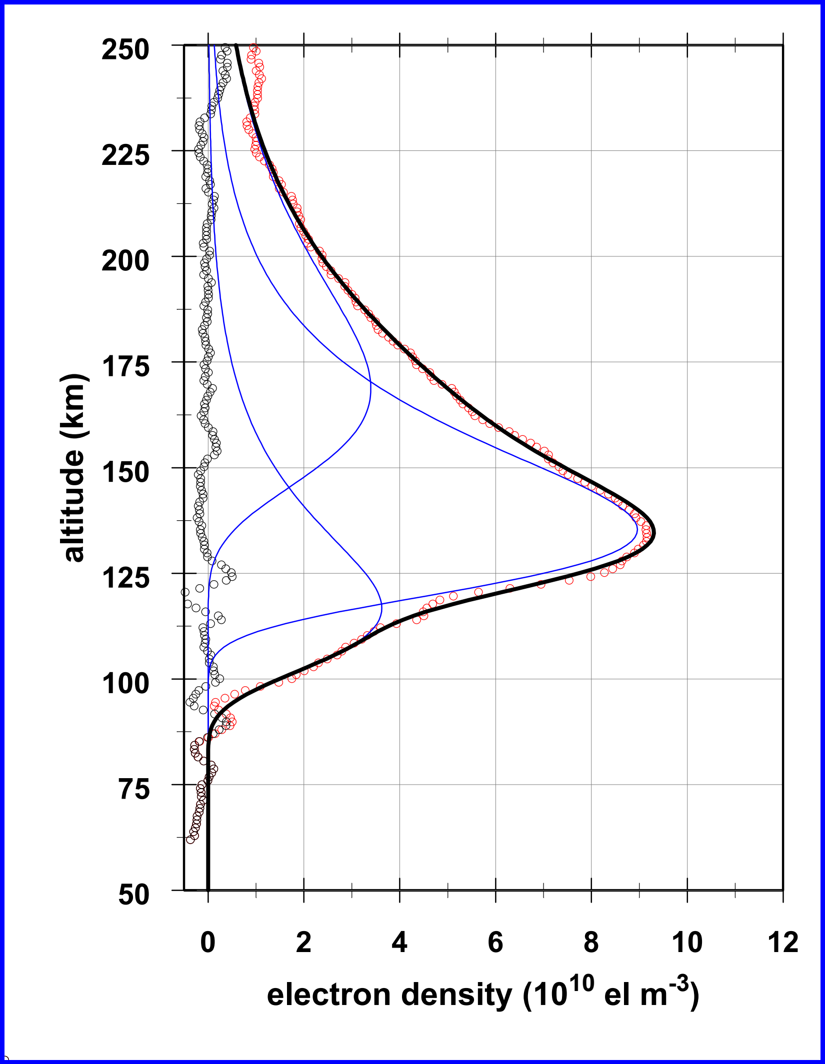

Why fit a Chapman Layer to the topside ionosphere?

- Shape described by only three parameters (N, z, H)
- Electron density decreases rapidly below peak altitude, decreases slowly above peak altitude. Any fit to the topside “step” must not affect electron densities around the ionospheric peak significantly.
- This mathematical function has been used previously to describe ionospheric regions controlled by photochemistry and regions controlled by diffusion
- This choice of fitting function does not imply that the topside “step” is a classical monochromatic, isothermal, photochemical Chapman layer.

Hypotheses

- Change in O/CO_2 ratio with altitude makes O^+, not O_2^+, the dominant ionospheric species. Subsequent change in recombination rate and/or diffusion coefficient affects electron density profile.
- Change in temperature with altitude affects scale height, which affects the change in optical depth with altitude and diffusion. Both of these can affect the electron density profile.
- Transition from photochemistry-dominated regime to diffusion-dominated regime.

Lack of Previous Observations and Theoretical Predictions

- Vertical resolution of Viking RPA measurements was ~5 km, so this “step” would be difficult to distinguish from the general trends in the topside.
- Mariner 9 and Viking Orbiter RS profiles are no longer available in digital format. Their noise level was 10^3 cm^{-3}, comparable with that of MEX and smaller than the MGS value of 3×10^3 cm^{-3}. This lack of detection is a puzzle.
- The scarcity of observations of the composition and temperatures of the Mars neutral upper atmosphere and ionosphere means that many model inputs are poorly constrained. In this situation, models are often tuned to reproduce existing observations, rather than fully explore the allowed regions of parameter space.

Conclusions

- A step, ledge, layer, or feature in the topside Mars ionosphere has been observed by MEX RS, MGS RS, and MARSIS.
- This is not visible in prior observations nor is it predicted by existing models.
- Hypotheses for the origin of this feature include vertical variations in chemistry, temperature, or the importance of photochemistry relative to transport.

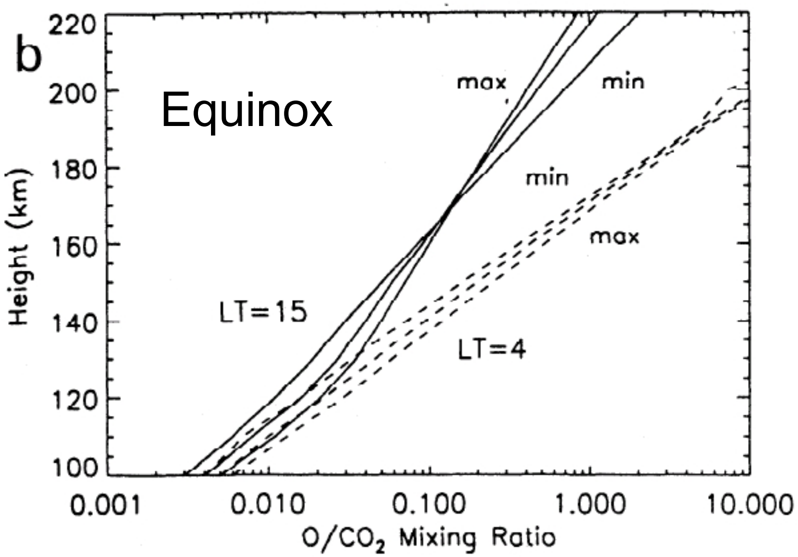

Figure 4. Mars Thermosphere General Circulation Model (MTGCM) equatorial fields and their variations over the solar cycle. (a) Mid-afternoon (LT = 1500, solid), and early morning (LT = 0400, dashed) temperature profiles over 100 to 220 km for SMIN, SMED, and SMAX cases; (b) midafternoon (LT = 1500) and early morning (LT = 0400) O/CO_2 profiles over 100 to 220 km for the same 3-EUV flux cases. At the F1-ionospheric peak (~130 km) at LT=1500, the O-mixing ratio varies from ~2-4% over the solar cycle. Mixing ratio curves are delineated as follows : LT=1500 (solid) and LT=0400 (dashed) for SMIN, SMED, and SMAX cases.

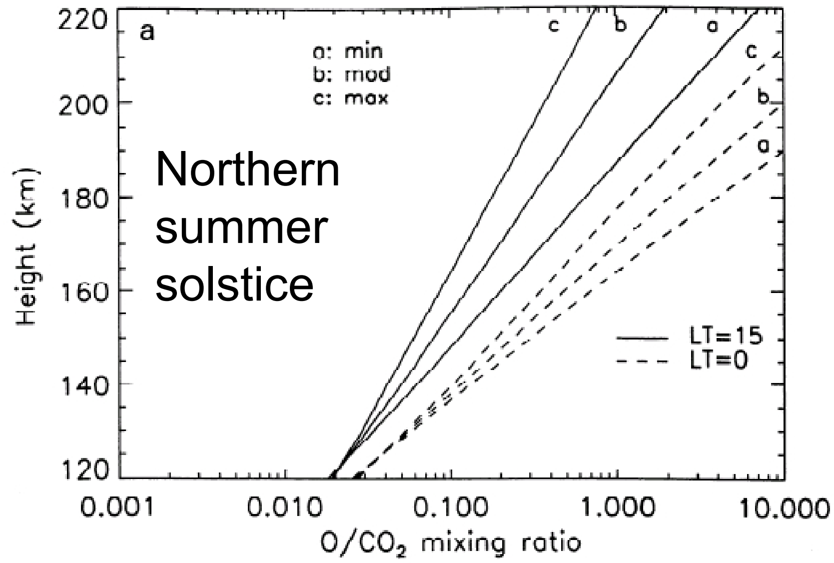

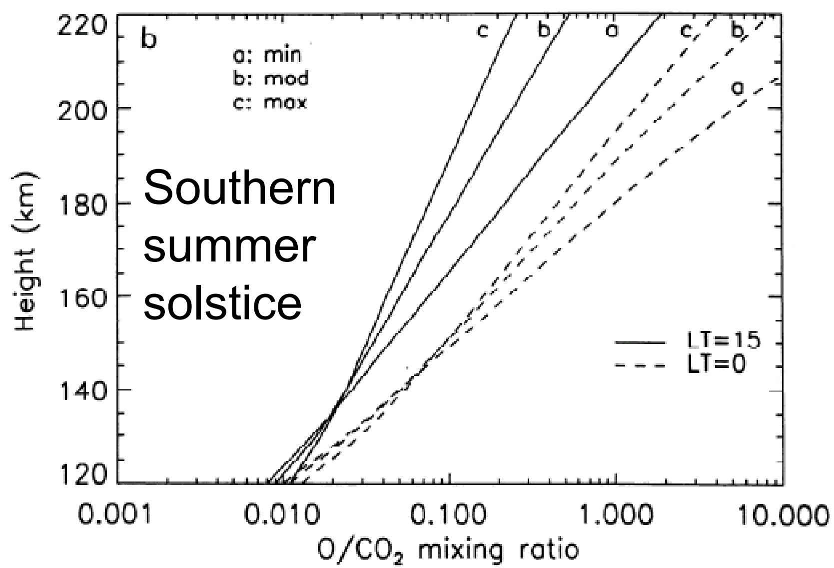

Figure 4. MTGCM subsolar latitude variations over the solar cycle for solstices. (a) Northern summer solstice (NSL): midafternoon (LT = 1500, solid lines), and midnight (LT = 0000, dashed lines) O/ profiles over 120 to 220 km for min, mod, and max cases. (b) Southern summer solstice (SSL): midafternoon (LT = 1500, solid lines), and midnight (LT = 0000, dashed lines) O/ profiles over 120 to 220 km for min, mod, and max cases.

Predicted O/CO_2 ratio varies greatly

Bougher et al. (1999, above) and (2000, right).

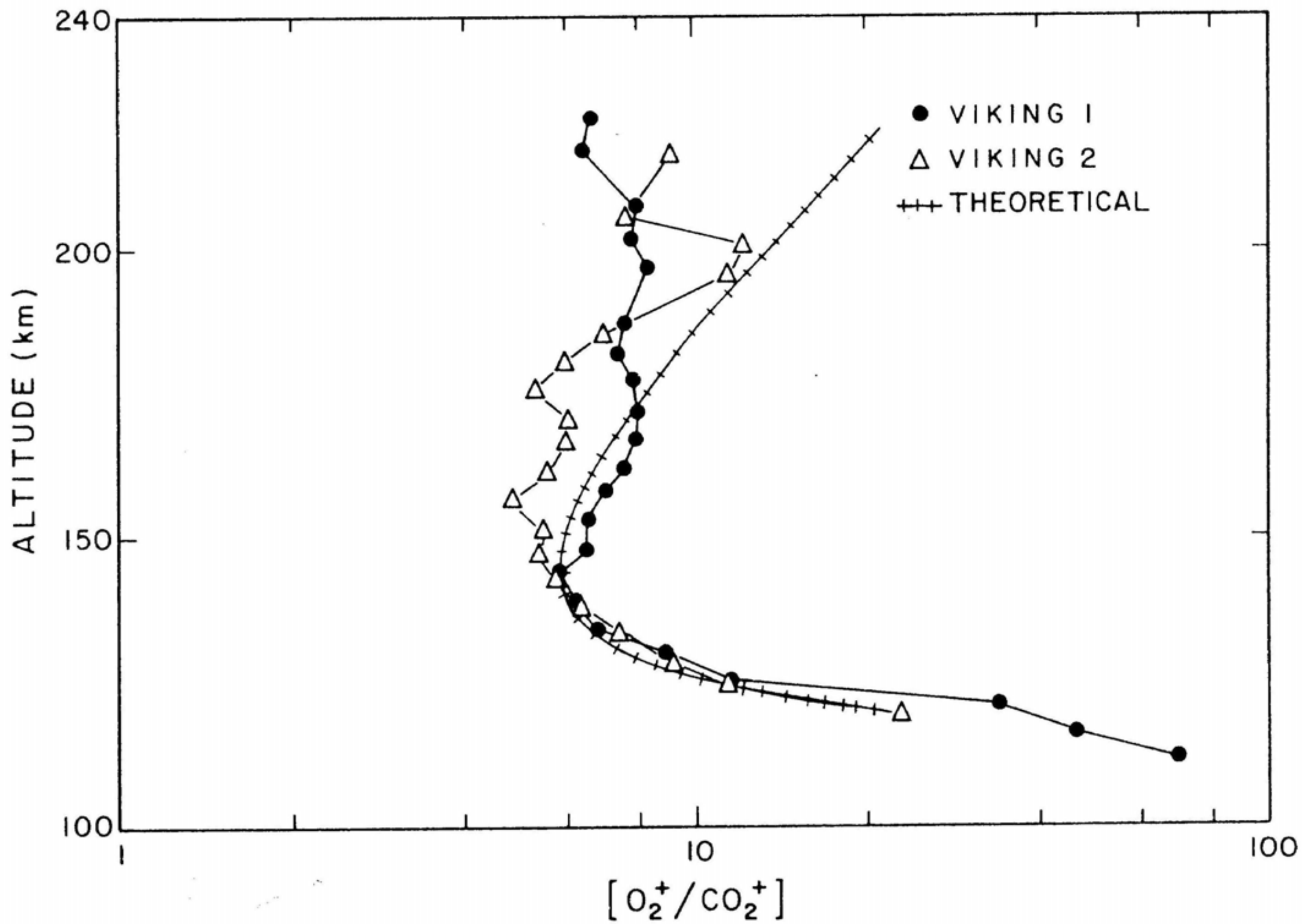

Fig. 9. Plots of the concentration ratio of O_2^+ to CO_2^+ measured from the two landers and determined from the model calculations presented in Figure 11.

The O_2^+/CO_2^+ ratio is affected by the O/CO_2 ratio
Hanson et al. (1977)

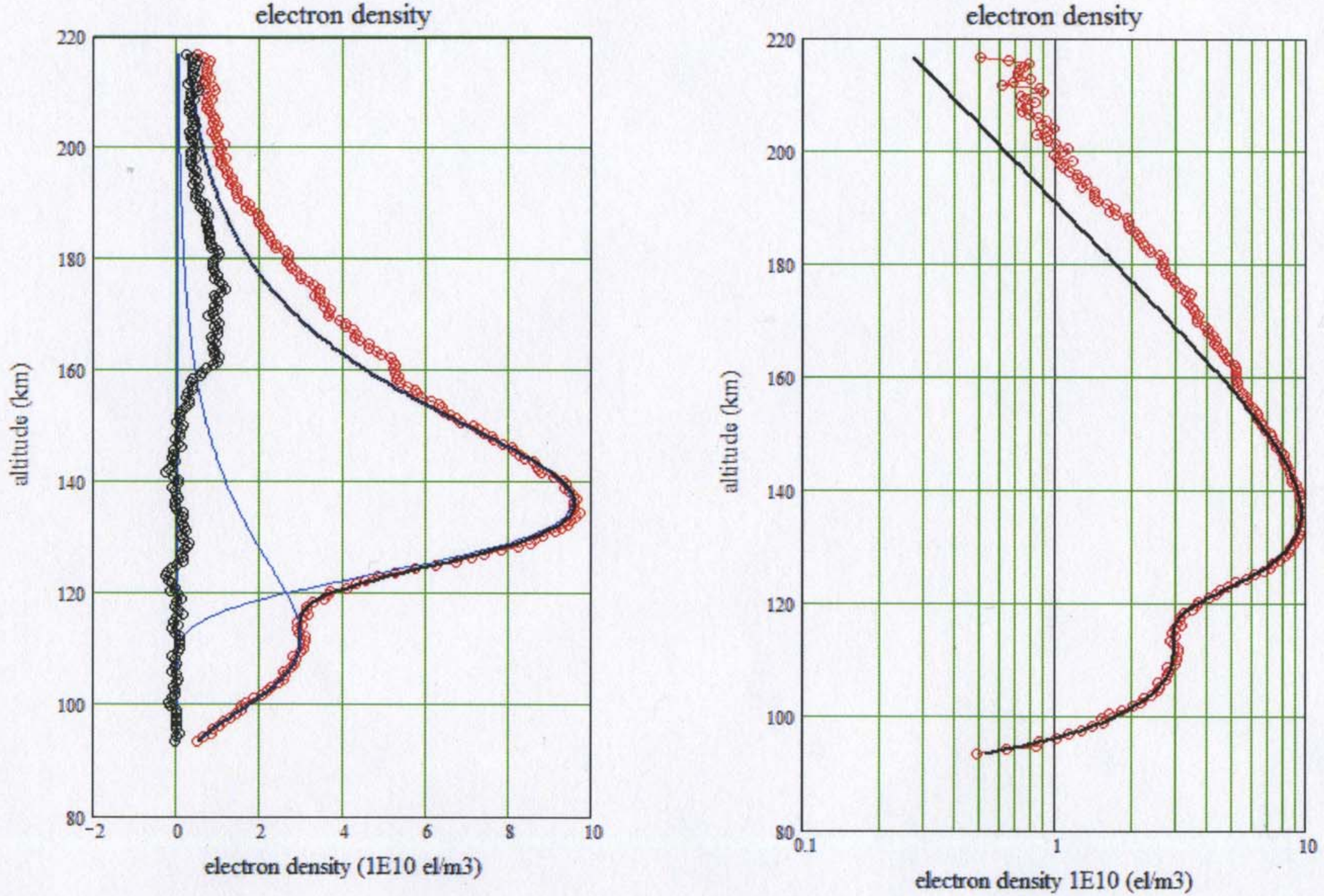
electron density
altitude (km)
electron density (1E10 el/m3)
electron density
altitude (km)
electron density 1E10 (el/m3)

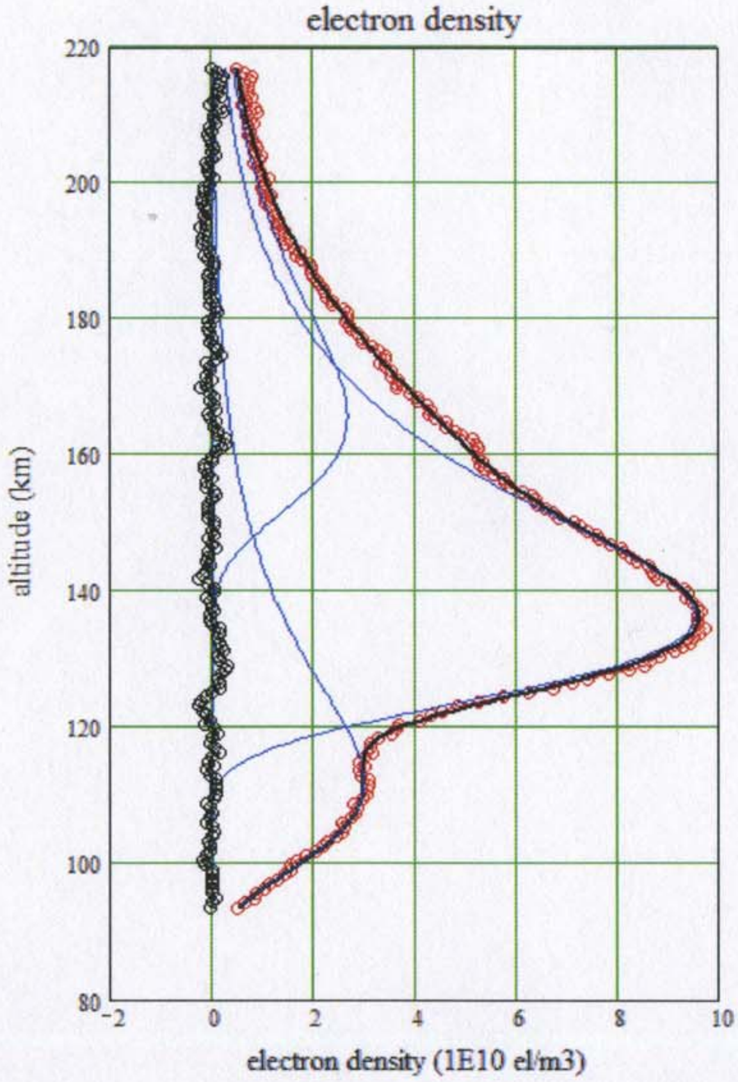
electron density
220
200
180
160
140
120
100
80
altitude (km)
-2
0
2
4
6
8
10
electron density (1E10 el/m3)

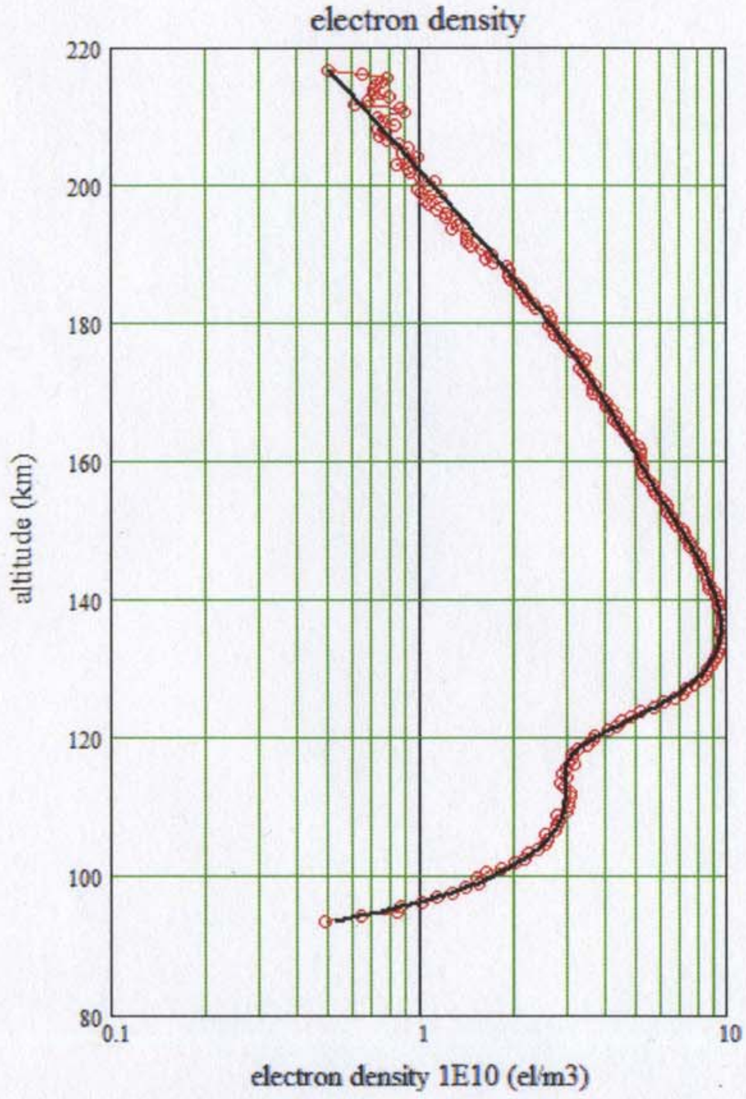
electron density
220
200
180
160
140
120
100
80
altitude (km)
0.1
1
10
electron density 1E10 (el/m3)

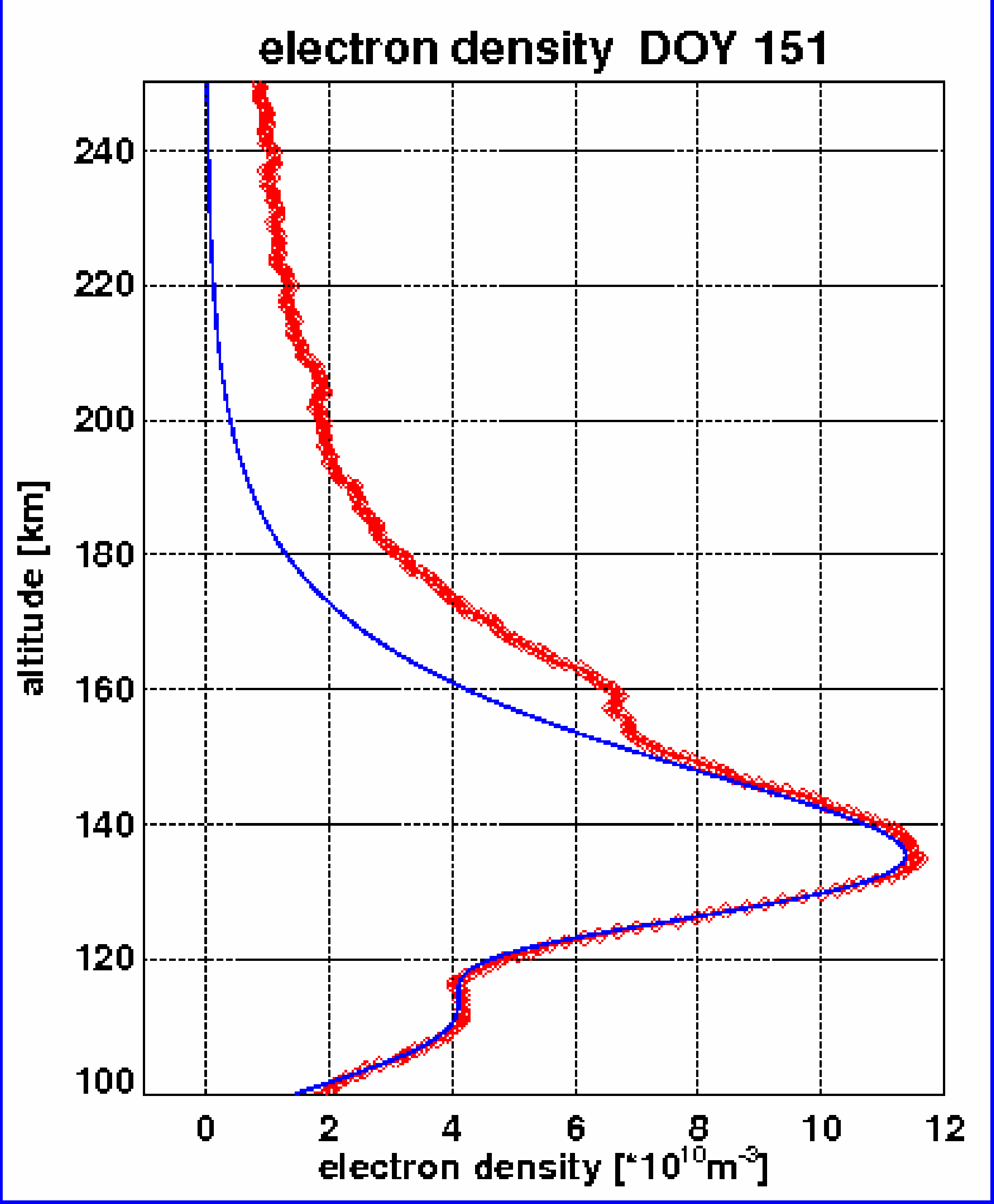

electron density DOY 151
altitude [km]
240
220
200
180
160
140
120
100
0
2
4
6
8
10
12
electron density [*10^10 m^-3]

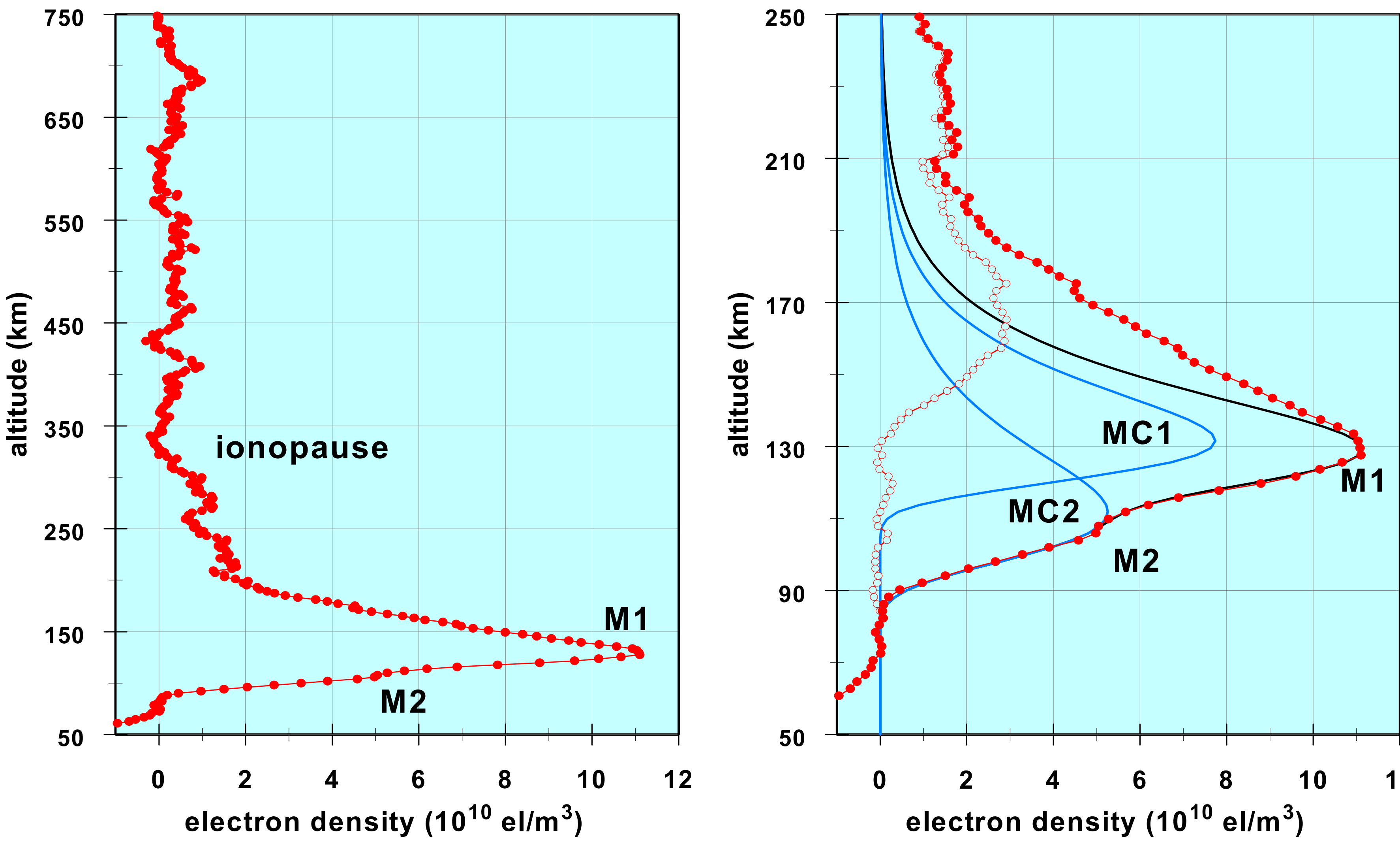

750
650
550
450
350
250
150
50
altitude (km)
ionopause
M1
M2
0
2
4
6
8
10
12
electron density (10^{10} el/m^3)
250
210
170
130
90
50
altitude (km)
MC1
MC2
M1
M2
0
2
4
6
8
10
12
electron density (10^{10} el/m^3)

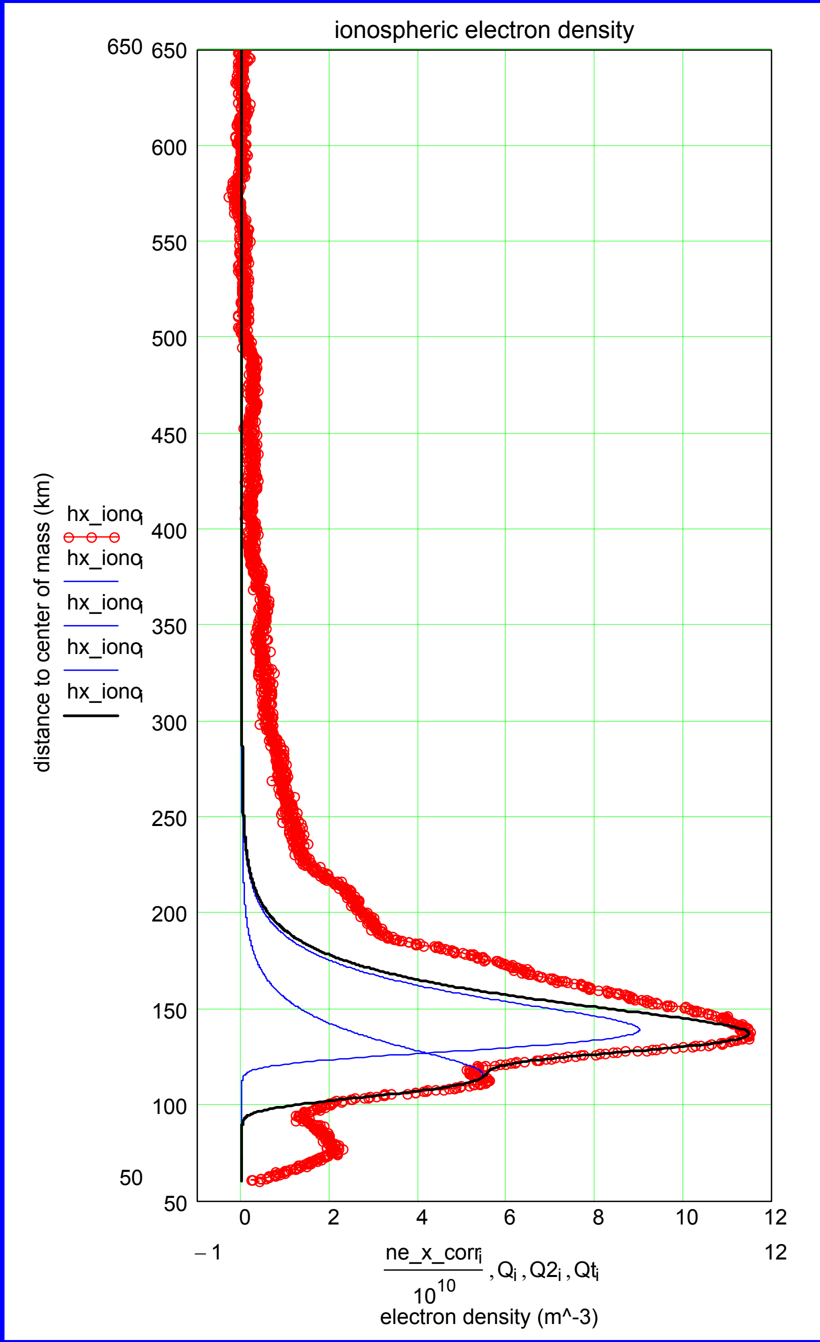

ionospheric electron density
650
650
600
550
500
450
400
350
300
250
200
150
100
50
50
distance to center of mass (km)
hx_iono
hx_iono
hx_iono
hx_iono
hx_iono
0
2
4
6
8
10
12
– 1
12
ne_x_corr_i / 10^10 , Q_i , Q2_i , Qt_i
electron density (m^-3)

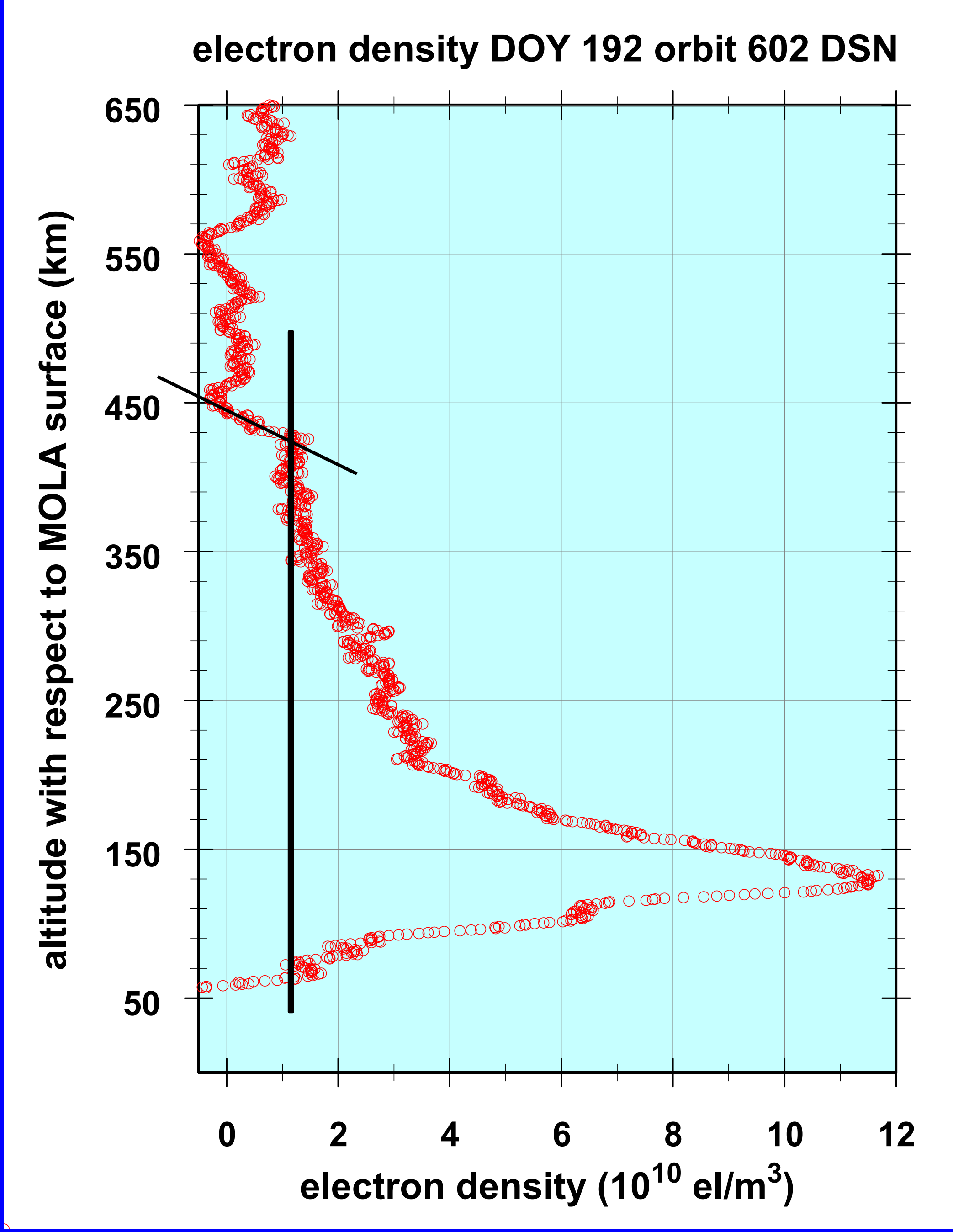

electron density DOY 192 orbit 602 DSN
650
550
450
350
250
150
50
altitude with respect to MOLA surface (km)
0
2
4
6
8
10
12
electron density (10^{10} el/m^3)

Introduction

Background

Previous Observations

Models

Topside Fits

Interpretation